Characterisation of iPSC-cardiomyocyte contractions using optical imaging

Otto Mulleners[1]*

Abstract
Congestive heart failure is a common illness affecting 1-2% of the population in developed countries. Due to the recent attempts to replace animal models, as well as the poor predictive value of animal models in heart failure. The development of a new *in vivo* heart model is critical for the development and testing of new drugs. The HeartCHIP project aims to develop such a model.
As part of the development process different analyses need to be developed for characterisation of heart muscle cells. For this purpose, more traditional methods such measuring the action potential can be used. But newer methods such as measuring the contraction by means of optical imaging are being developed and tested.
In this paper, image analysis characterisation of cardiomyocytes and vascular smooth muscle cells are explored. Using images recorded from transmission light as well as fluorescent beads the movements of a monolayer of cells is tracked and analysed. Next to this, the potential for live cell imaging of actin structures during contraction is explored, allowing the study of sarcomere compaction during contraction.

[1] *Department of Molecular genetics, Erasmus Medical Centre, Rotterdam, The Netherlands and Faculty of Applied Science, Delft University of Technology*

Contents

Introduction

0.0.1 Heart failure

One of the leading causes of death in developed countries with a prevalence of 1-2% is heart failure[CDC, 2015]. Heart failure is a chronic, progressive disease characterised by the inability of the heart muscle to meet circulatory demands. This causes an enlarged heart with an increased beating rate to provide sufficient oxygen to the body, eventually resulting in total inability of the heart to properly provide the body with blood and oxygen[Heartchip, 2015, McDonagh et al., 2011].

0.0.2 Cardiomyocytes

Heart muscle cells, otherwise named cardiomyocytes, are the cells that make up most of the heart. When a patient suffers of heart failure these are the cells that get affected. Cardiomegaly, an enlarged heart, is a result of overexertion of the heart, causing the sarcomeres to slip and slowly have less and less overlap. This overlap is needed for proper contraction. Cardiomegaly generally results in a vicious circle of overexertion where less overlap of filaments causes a higher heartbeat and force required which causes even less overlap, etcetera often requiring lifelong medical treatment.

0.0.3 Striated muscle cells

Cardiac muscle is a type of striated muscle, which contains regularly repeated subunits, sarcomeres. These are presented as bands in the muscle fibres.

A single sarcomere runs from Z-disk to Z-disk. The Z-disks are composed of α-actinin and are used to anchor actin and titin filaments. In between the actin filaments, attached to titin, are myosin filaments. In figure 1 a single sarcomere

is shown. During contraction myosin 'walks' over the actin filament towards the Z-disks in both directions. This causes compaction of the sarcomere and increased overlap between the myosin and actin filaments (fig. 2).

Figure 1. Sarcomere structure, *adapted from [Hall and Guyton, 2016] fig. 6-3*

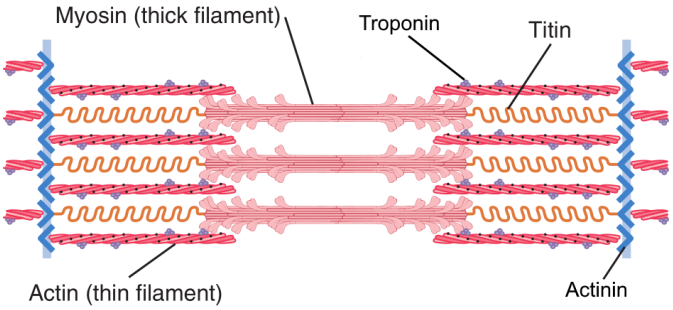

Figure 2. Sarcomere compaction during contraction [Hall and Guyton, 2016] fig. 6-8

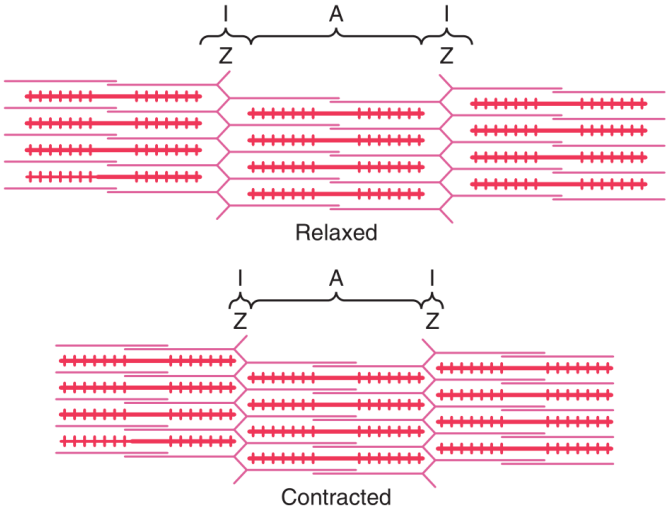

To allow the myosin to walk over the actin, calcium ions need to be present. Calcium ions bind the troponin complex, which is attached to the actin filament. When calcium binds to troponin a conformational change occurs, which in turn changes the tropomyosin configuration. The tropomyosin covers active sites on the actin filaments that myosin can bind to. This way calcium regulates contractions, making it an essential part of muscle function.

The leading model, the *sliding filament model* as proposed in 1953, describes the precise way sarcomeres contract. In figure 3 a schematic representation of the myosin (MF), myosin heads(blue oval) and actin(AF) is presented. Contraction consists of a cycle of repeated steps by the myosin heads. The ATP is hydrolysed to ADP and a free phosphate, the myosin heads rotates toward the actin filament. When the head is close enough to the actin, the myosin binds weakly to an active site. The free phosphate is released. The energy released by this allows the myosin head to rotate back into the first configuration,

Figure 3. Sliding filament model[Krans, 2010]

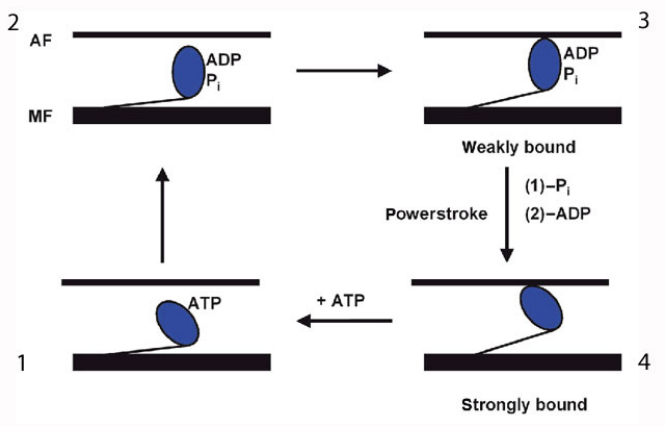

thereby strongly binding to the actin. Finally, the myosin only releases the actin upon binding a new ATP molecule which causes the process to repeat, as long as active sites are available [Krans, 2010, Stewart et al., 2013, Geeves et al., 2005].

0.0.4 Cardiomyocyte beating

Cardiomyocytes contract due to a fluctuation of the membrane potential, the cardiac action potential. This is the cycle of changing membrane potential which causes the specific opening and closing of ion-channels needed for controlled contraction of the sarcomeres. The main channels involved cause influx and efflux of Na^+, K^+ and Ca^{2+} ions. The cardiac action potential development can be divided into 5 phases(fig.4) [Hall and Guyton, 2016].

Phase 0 Rapid depolarisation (potential becomes positive) of the cell membrane. This is achieved by the opening of fast voltage gated Na^+ channels, when the membrane potential has risen from ~-90 mV to ~-70 mV. Opening of the Na+ channels causes the membrane potential to rapidly increase to ~+20 mV. This phase is the start of the contraction.

Phase 1 Sodium channels close due to the voltage increase, which allows a slight repolarization of the cell membrane.

Phase 2 The potential plateaus due to opening of calcium influx pumps (slowly during phase 0 and 1) and the closing of potassium efflux pumps, which balance the ions inside and outside the cell such that the action potential remains relatively stable.

Phase 3 Calcium channels close while the potassium efflux channels open again causing the membrane potential to drop to the resting potential again. This is where the relaxation begins.

Phase 4 This is the resting membrane potential, ~-90 mV. Although this is the commonly accepted cardiac action potential cycle, for beating stem-cell derived cardiomyocytes this would be impossible, because this doesn't explain the automaticity exhibited. This progression requires a nerve or sinoa-

trial node to provide the necessary action potential for sodium channel opening. Most likely, during phase 4, similarly to pacemaker cell potential, calcium slowly enters the cell. This causes a slow depolarisation of the membrane to the necessary ~-70 mV for the sodium channel to open[Kim et al., 2015].

Figure 4. Cardiomyocyte action potential development during a single beat [Hall and Guyton, 2016] fig. 9-4

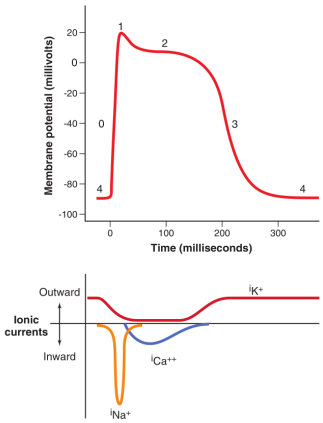

The action potential reaches into T-tubules. These are extensions of the cell membrane reaching deep into the cell, wedged in between myofibrils. The potential in the T tubules causes opening of calcium channels. Calcium entering the cell causes the release of more calcium from the sarcoplasmic reticulum. The calcium can bind troponin and this causes contractions in the sarcomeres. At the end of phase 2 of the cardiac action potential, the calcium influx is cut off and calcium is actively pumped out of the cell and into the sarcoplasmic reticulum. This is done by a Ca^{2+}-ATPase pump, which exchanges the calcium with sodium. This sodium is subsequently exchanged for potassium using a Na^{+}-K^{+}-ATPase pump (figure 5)[Hall and Guyton, 2016, Ibrahim et al., 2011].

Figure 5. Cardiomyocyte contraction pathway [Hall and Guyton, 2016] fig. 9-6

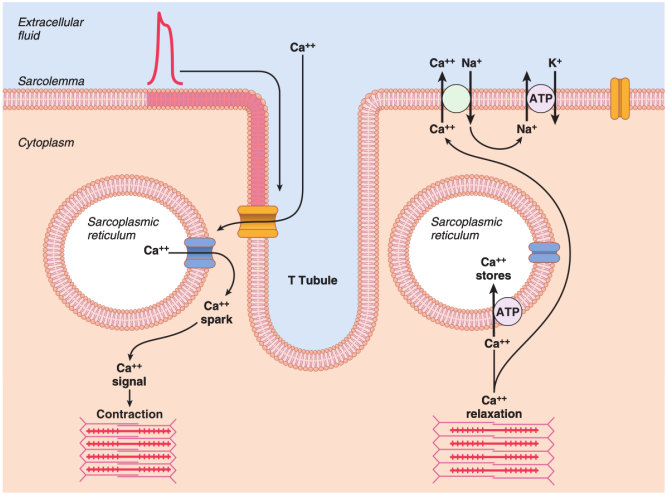

Figure 9-6. Mechanisms of excitation-contraction coupling and relaxation in cardiac muscle. ATP, adenosine triphosphate.

0.0.5 Smooth muscle cells

Smooth muscle cells do not contain sarcomeres. Instead there are bundles of actin anchored to the cell membrane by dense bodies, mainly composed of α-actinin. Actin bundles are bound to myosin filament which pulls on the actin through a sliding filament mechanism to contract the cells [Brozovich et al., 2016].

Vascular smooth muscle cells do not generally contract in vitro, because of the lack of stimuli and in contrast to cardiac cells these cells do not exhibit automaticity. But using an external stimulus, it is possible to make them contract. Similar to how cardiac cells naturally beat, using a high potassium solution as medium, potassium will diffuse into the cell and depolarize the cell membrane. This causes opening of the voltage-gated Ca^{2+} channels which causes an influx of calcium-ions.

Smooth muscle cells do not contain Troponin, instead the calcium-ions bind calmodulin (CaM) which activates myosin light chain kinase (MLCK), which phosphorylates myosin heads. This causes the cycling of attachment and detachment of the myosin heads. During relaxation Ca^{2+} channels pump the calcium out of the cell, causing inactivation of MLCK. Myosin phosphatase is needed to dephosphorylate the myosin heads to stop the filaments from sliding.[Somlyo and Somlyo, 1994, Waugh, 1962, Yeung et al., 2017]

Figure 6. Smooth muscle cell contraction pathway [Hall and Guyton, 2016] fig. 8-3/5

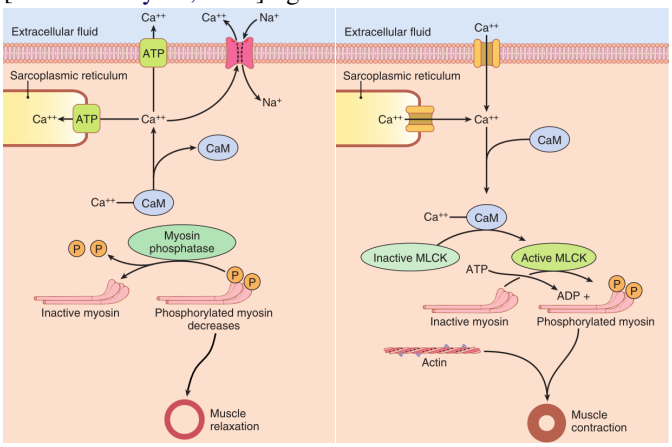

0.0.6 PDMS

PDMS, Polydimethylsiloxane, is a type of silicone. PDMS is colourless, odourless, chemically inert and fire-resistant, insoluble in water and hydrophobic. These properties make them ideal for use with live cells. And apart from those properties depending on the curing ratio, time and temperature the compound allows for altering the elastic modulus range from $10^2 - 10^5$ Pascal [Gutierrez and Groisman, 2011]. This elasticity can be exploited for the characterisation of contractions using microscopy.

For the project two assays using PDMS were considered. First, an array of PDMS micropoles (2 μm diameter).7 These

micropoles are coated with ECM proteins such as fibronectin, and cardiomyocytes are grown on top of these poles.

By studying the deflection of the poles, the contraction force can be calculated using slender beam theory[Beussman et al.

The assay used in the project was developed by Ibidi. Microscopy slides containing wells within wells, the inner wells can be filled with a layer of PDMS to provide a flexible surface for the cells to beat upon and deform the PDMS.

Different elasticities can be produced in this layer, enabling the study of contraction force of cardiomyocytes.

Figure 7. SEM image of an epithelial cell adhering to a micropole array. [Chown and Kumar, 2007] fig. 5A

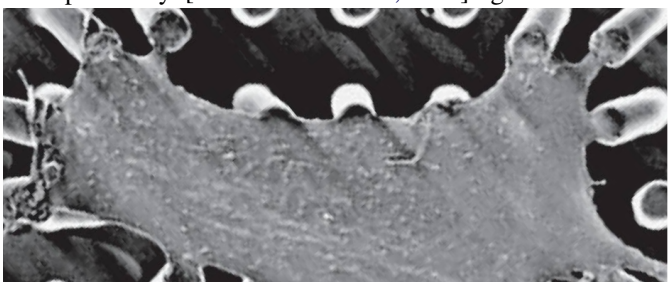

Figure 8. Section of Ibidi μ-slide angiogenesis with PDMS as substrate gel.
Figure adapted from http://ibidi.com

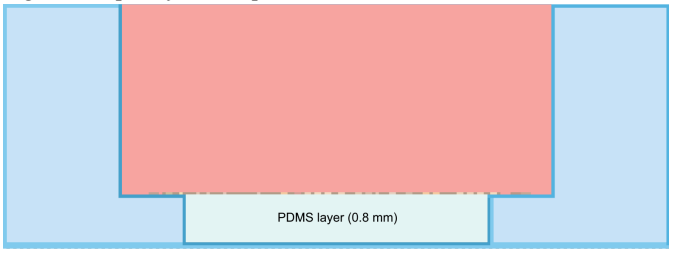

0.0.7 Project

This project is executed as a part of the HeartCHIP project. This project aims to develop a new in vitro heart failure model for testing new drugs as well as testing drug efficacy using Organ-on-a-chip technology. Current models do not mimic the heart well, nor do animal models provide sufficient predictive value. Part of the project is to integrate non-destructive microscopy into the model for prolonged drug functionality and efficacy monitoring.

Microscopic image analysis is often overlooked by biologists despite bearing greater and greater significance over the past decades. The author provides a primer on what might be possible on the image analysis side of the HeartCHIP project. In the duration of the project attempts have been made at growing and filming their own Cardiomyocytes, analysing the videos provided by Ibidi and as an outing outside of the (direct) scope of the HeartCHIP project growing of vascular smooth muscle cells.

For the project Ibidi has provided the PDMS surfaces to grow the cells on, as well as videos recorded by their own researchers earlier. Pluriomics have provided the Cardiomyocytes and the medium to grow them to healthy mature cells.

1. Methods and Materials

1.0.1 PDMS microarrays

To produce the PDMS micropole arrays dr. E. Mendes (Chemical engineering, TU Delft) provided the SU-8 photoresist master stamp, with 1.5, 2.5 and 3 μm diameter micropoles.

The master is used to cast a negative mould from PDMS which in turn is used again to cast the arrays. The PDMS structures were cast by K. Zhang, MSc (Under supervision of dr. E. Mendes, Chemical engineering, TU Delft). The PDMS was mixed at a ratio of 10:1, polymer to curing agent, allowed to degas for 1 hour and cured at 68°C for 24 hours. To prevent permanent bonding between the negative mould and the second cast, the negative mould was passivated using silane gas.

Figure 9. Illustration demonstrating the manufacturing of a PDMS cast [Sniadecki and Chen, 2007] fig. 2

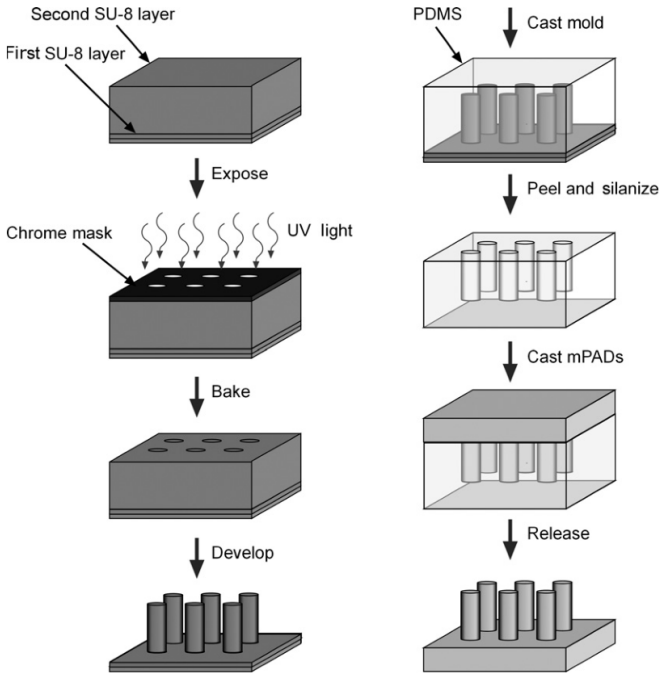

1.0.2 Coating of PDMS microarrays

The coating of the PDMS micropole arrays happened using a flat piece of PDMS as a stamp. The flat pieces are cut into 1x1cm pieces to match the micropole array size. Subsequently fibronectin aliquots of 50 μl of the stock solution (50 μg/ml) were spread onto the centre of the flat PDMS and allowed to hydrophobically adsorb for 1 hour to saturate the stamp surface. The excess fibronectin is washed off using MilliQ water and the stamp is dried with N_2. The micropole arrays are placed into the UV Ozone-plasma cleaner for 7 minutes which renders it temporarily hydrophilic[Özçam et al., 2014]. The flat stamps are placed gently but firmly on top of the

micropoles to allow fibronectin transfer through hydrophilic interactions for a few minutes. After the stamping, the micropole arrays are sterilised using 100% & 70% ethanol and treated with 0.2% Pluronics F-127 to prevent cell adhesion to the sides of the poles. This leaves micropoles coated with extracellular matrix protein on the tip and Pluronics on the side to allow for cell adhesion to the tips, but inhibiting adhesion to the sides and bottom. The PDMS is placed onto normal culture plates in the appropriate medium and ready for seeding the cells.[Sniadecki and Chen, 2007, Beussman et al., 2016]

Figure 10. Illustration demonstrating the stamping of ECM onto the poles [Sniadecki and Chen, 2007] fig. 4

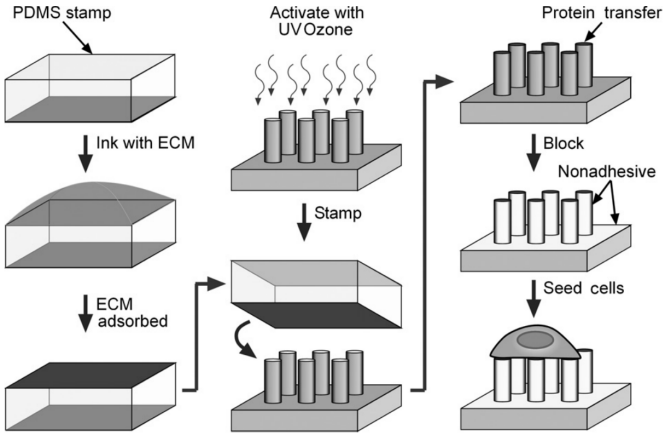

1.1 Vascular smooth muscle cells

Before growing cardiomyocytes, there were several cell culturing techniques to get acquainted with. Since the cardiomyocytes weren't capable of surviving trypsinisation. And there were only a limited number of cardiomyocytes available, there was a need for a different cell line to be practiced upon before moving onto the cardiac muscle cells. The cells used were Vascular Smooth Muscle cells from the aortas of the Fibulin 4 mouse model. This mouse model has been developed by the Erasmus MC to exhibit Fibulin 4 under expression which causes differences in the actin organisation in the cell[Hanada et al., 2007].

1.1.1 Medium

To a bottle of 500 ml DMEM (4.5g/L glucose, with Ultraglutamine-1, BioWhittaker), 50 ml Fetal calf serum (Biowest, South America origin) and 5 ml of Penicillin-Streptomycin (6 mg/ml resp. 10 mg/ml, Gibco) are added.

1.1.2 Thawing

First place the amount of medium required into the water bath until it has reached 37°C. To thaw the VSMCs, the vial is taken from the liquid nitrogen freezer and thawed in the water bath at 37°C. When fully thawed add the vial to 5 ml of medium also at 37°C. Put the tube into the centrifuge for 5 minutes at 1000 revolutions per minute. This was the DMSO used for freezing can be taken out of the cell suspension. Aspirate the supernatant. Add 10 ml of fresh medium to the pellet and suspend by pipetting up and down for at least 3 times.

The vial contains the contents of exactly 1 confluent 100mm dish of cells, to allow the cells to grow only part of the suspension should be plated. Depending on when the cells were needed again, for the VSMCs anywhere between 1:10 and 1:30 of the suspension was used for plating. Add the cells to plates coated with 0.1% gelatine for at least half an hour, and add medium to make the total amount of medium 10 ml for a 100mm plate. Make sure the cells are homogeneously spread over the plate before putting them in the incubator at 37°C and 5% CO_2.

1.1.3 Cell passage

First place the amount of medium required, D-PBS and trypsin into the water bath until they have reached 37°C. To passage the VSMCs, the full plates containing the cells are taken out of the incubator and washed with 5 ml D-PBS 2 times in a row, until the D-PBS no longer shows a pink hue.

Next 1 ml of trypsin is pipetted onto the 10cm plates, and spread homogeneously over the surface by swirling. The plates are put back into the incubator for 10 to 15 minutes, benefiting from direct heat of the incubator shelf instead of being stacked.

After 10 minutes check whether the cells have dissociated from the surface of the plate. When the cells have released it can be clearly seen on the microscope, and checked by swirling the dish to see if all cells move with the liquid. The cells need to be resuspended to break up clumps. And the trypsin is deactivated by FCS in the medium which contains protease inhibitors.

To resuspend the cells 5 ml of medium is added and pipetted up and down, flushing the plate surface repeatedly. After adequate resuspension, the 6 ml are placed into a tube and into the centrifuge for 5 minutes at 1000 rpm. The supernatant is aspirated and the pellet is suspended in 10 ml medium. Finally, the cells are diluted and plated like above.

1.1.4 Freezing

For freezing the cells, nearly the exact same protocol as for passaging is used. For freezing the final suspension is not suspended in 10 ml medium, instead 1 ml is used. This medium contains 10% DMSO to serve as a cryoprotectant[Xu et al., 2007]. The suspension is pipetted into a 1.5 ml cryotube. To freeze the cells are place in the −20°C freezer until frozen, moved to the −80°C until frozen and into a liquid nitrogen tank until needed.

1.2 Cardiomyocytes

The cardiomyocytes were pluricyte®iPSC derived cardiomyocytes (Pluriomics® PCK-1.5) [Den Hartogh and Passier, 2016] supplied by Pluriomics® together with pluricyte® cardiomyocyte medium (Pluriomics® Cat# PM-2100-150mL).

1.2.1 Fibronectin coating

Fibronectin is a biological extracellular matrix protein which contains the RGD motif which allows cells to adhere to the

Table 1. Table specifying coating volumes to be used

Plate format	Volume
μ-slide angiogenesis (Ibidi)	50 μl
8 Well Chamber removable (Ibidi)	400 μl
8 Well Chamber glass bottom (Ibidi)	400 μl
12-well plate	1000 μl

culture plates. Start with diluting the fibronectin stock solution (1mg/ml), in D-PBS (incl. Ca^{2+}/Mg^{2+}) to get a 10μg/ml fibronectin coating solution and mix the solution carefully. **Nb** Sometimes a 5 times higher concentration yielded better results in Ibidi tests. Plate the coating solution immediately onto the plates (see Table for coating solution volumes) and incubate the fibronectin-coated plate in a cell culture incubator at 37°C, with 5% CO_2 for 3 hours. Incubation for longer times are not deleterious unless the solution dries out. It can also be left to polymerise overnight at 4°C. Finally aspirate excess fibronectin coating solution right before plating the cells.

1.2.2 Matrigel coating

Matrigel™is a biological extracellular matrix protein mixture which contains fibronectin amongst others, which also allows cells to adhere to plates and is sometimes favoured over different adherence preparations.

An aliquot of matrigel™was thawed and kept on ice. Using a frozen pipette tip to add the aliquot to a 15 ml tube, and a 10-ml pipette to add the required volume of cold DMEM/F12 to dilute to the matrigel 1:100. In some cases a 1:20 solution provided better results in Ibidi tests, especially when coating PDMS. But with higher concentrations extra care should be taken not to leave to much matrigel™when aspirating. Plate the matrigel™coating solution immediately onto the plates (see Table for recommended coating solution volumes) and allow for polymerisation for at least 30 min at 37°C, 60 min at room temperature or overnight in the fridge **Nb** Longer incubation at 4 C is acceptable if the gel doesn't dry out. To prevent this sterile water can be added to the space between wells. Finally, Aspirate as much of the excess matrigel™coating solution as possible, right before plating the cells.

Nb matrigel™polymerises above 10°C, so it should be kept at 4°C or on ice while working with it.

1.2.3 Seeding

The plates were coated in matrigel™and Fibronectin as described above. Six ml medium is warmed to room temperature and mixed by inverting the flask. The vial of Cardiomyocytes is retrieved from the liquid nitrogen storage and placed in the incubator at 37°C for 4 minutes. Gently transfer the contents of the vial to a 50 ml tube using a p1000 pipet. Avoid pipetting up and down to agitate the cells as little as possible. Rinse the empty vial with 1 ml medium (room temperature) and add the 1 ml medium drop wise to the 50 ml tube containing the cells, add 1 drop every 5 seconds using a p1000 pipette while gently swirling the cells after each drop. Now using a 5 ml pipette 4.7 ml of medium is added dropwise every 2 seconds. Count the cell concentration as described below. Determine the dilution factor to reach the desired concentration and add medium to the cell suspension accordingly. Aspirate the matrigel™/fibronectin from the culture plates and plate cells according to table making sure to transfer the cells extremely gently. Place the cells in the incubator at 37°C. The medium should be replaced the first day after seeding and every other day after that. First contractions might be seen 24-48 hours after thawing and stable beating monolayers should be observed between 7-12 days post-thaw.[Pluriomics,]

Table 2. Table specifying volume and cell number to plate

Plate format	Cells per well
μ-slide angiogenesis (Ibidi)	15.000
8 Well Chamber removable (Ibidi)	75.000-150.000
8 Well Chamber glass bottom (Ibidi)	75.000-150.000
12-well plate	200.000-400.000

1.2.4 Haemocytometer

Cells were counted using a Fuchs Rosenthal Counting Chamber. To count the cells 20 μL of the cell solution was centrifuged at 250g for 3 minutes. The pellet was resuspended in 1 ml medium. +-8 μL of the 1ml is pipetted between the haemocytometer and the coverslip. To count the cells the red square in the figure is used. Three or four squares should be counted and averaged. After which the average number of cells is multiplied by 104 which gives the concentration of the original cell solution in cells/ml.

Figure 11. Haemocytometer grid. Red square is 1mm^2 [Commons, 2007]

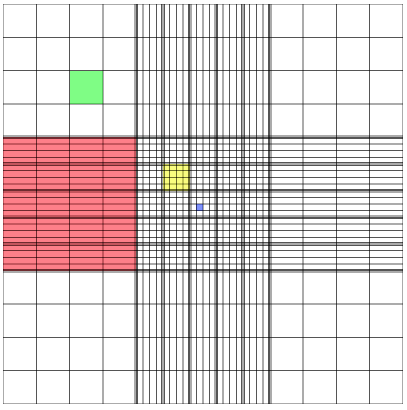

1.3 Immunofluorescence

1.3.1 Fixed cell

For the immunofluorescent staining and fixing of the cells the following protocol was used. First, a PBS (10x) stock solution was prepared. The following ingredients were dissolved in 800 ml MilliQ water.

Table 3. Ingedrients for PBS and PBS+

PBS 10x	
Volume/Mass	Component
800 ml	MilliQ (Millipore)
80 grams	Sodium Chloride
2 grams	Potassium Chloride
14.4 grams	Na_2HPO_4
2.4 gram	KH_2PO_4

PBS+	
Volume/Mass	Component
100 ml	PBS 1x
0.5 grams	BSA (Sigma-Aldrich)
0.15 grams	Glycine (Sigma-Aldrich)

For the PBS, the pH is adjusted to 7. And the volume is filled to 1 litre. For fixing the cells first the plates were washed with PBS(1x) after which 2% Paraformaldehyde in PBS(1x) was added to the plates for fixing the cells for 15 minutes. The cells are then permeabilized with Triton X-100 (0.1% in PBS(1x)) washing 3 times and immediately taking the solution off, and washing 2 times leaving the solution on the cells for 10 minutes. Wash with PBS+ for 30 minutes. For the staining, the PBS+ is removed and the area around the coverslip has to be completely dried. Aliquots of 100 μl of the primary antibodies are added to the coverslips. Dilution of the antibodies is usually 1:1000, but depends on the antibody. For troponin-I and alpha-actinin 1:250 was used. This is left overnight in a humidified container at 4°C. Before adding the secondary antibody, the coverslips are washed again using Triton X-100 (0.1% in PBS(1x)). Wash 3 times and aspirate immediately, and wash 2 times leaving the solution on the cells for 10 minutes. Wash with PBS+ shortly. For the secondary antibody again dry around the coverslip and add 100μl to each slide. Making sure to write down which animals the primary antibodies were produced in, to match the right fluorescence on the microscope.

From this point forth the slides should be kept in the dark. Leave the secondary antibodies to work for 1 hour. Then wash with Triton X-100 (0.1% in PBS(1x)) 3 times and immediately aspirate, and wash 2 times leaving the solution on the cells for 10 minutes. Wash with PBS(1x) shortly. Finally dry the coverslips as well as possible without touching the surface and add 1 drop (<10 μl) of Dapi-Vectashield to the coverslip before putting it onto the microscope slide. Finally wait for the slides to be completely dry before sealing the coverslip using nail polish.

1.3.2 Live cell

For the staining of live cells, SiR-actin (Cytoskeleton, inc.) was used. A solution of 80 nM SiR-actin was made, diluted in the appropriate medium. After preparation of the staining solution, the regular cell medium is replaced by the solution and left in the incubator at 37°C overnight. The next day microscopy can be performed using Cy5 settings.

1.4 Microscopy

1.4.1 Confocal

Fixed cell imaging of the cardiomyocytes and smooth muscle cells were performed using a Leica SP5 AOBS microscope utilizing a 63x oil immersion lens (1.40 NA, HCX PL APO CS, Leica). The fluorophores were excited using the 405, 488, 594 and 633 laser lines. And recorded by 2 photomultiplier tubes and a Hybrid Detector. The resulting images were analysed in ImageJ and the maximal z-projection was used for the final image construction.

1.4.2 Widefield

Live cell imaging of the cardiomyocytes and smooth muscle cells were performed at 37°C and 5% CO_2 (Tokai Hit GM-8000) in a small water bath incubator. The microscope used was a Nikon Ti-eclipse inverted microscope using a 20x dry lens (0.75 NA, PLAN APO lens, Nikon). For the transmission light images, a halogen lamp was used and a mercury lamp in the far-red spectrum for SiR-actin excitation. The videos were taken by a Photometrics Coolsnap HQ2 1390x1040 pixels 14bit cooled CCD camera. And recorded using Metamorph Imaging software. For the smooth muscle cell contraction under the widefield microscope the medium needed to be replaced with a solution high in Potassium to induce contractions in the VSMCs. Three concentrations and 2 different fluids were used. DMEM and D-PBS for dissolving 60, 120 and 240 mM potassium chloride. The quickest to perform the replacement is to replace half the medium present, such that these solutions resulted in 30, 60 and 120 mM potassium chloride concentrations.

Due to the steps required after turning on the camera, setting the camera to record for approximately 5 seconds longer than the video is advised. To induce the contractions, it is necessary to perform the following steps as swiftly as possible as well as try not to agitate the medium much.

Initially, about half of the medium is aspirated using a long 5ml pipette tip placed onto a syringe. An electrical pipette creates too much current in the liquid. Next the medium was filled back up by KCl in DMEM, again using the syringe with the pipette tip to prevent current and have a long reach so that the microscope can stay in the same position and keep filming.

If the cells show contraction these should occur within a few minutes or less.

1.4.3 Particle tracking

For particle tracking the SOS plugin for ImageJ, written by dr. Ihor Small was used[Reuter et al., 2014]. The first analysis technique used for analysis of the cell contractions is particle tracking. Particle tracking involves spot detection in an image series and following the position of the particle over the duration of the video. To perform particle tracking, the particles need to be detected in each image, and subsequently linked to their most likely past/future self in the next frame.

Spots are detected by performing a weighed least-squares Gaussian fitting of point spread functions, with supplied sigma

Table 4. Table showing the antibodies and fluorophores used

	Primary antibody	Fluorophore	Excitation/emission (nm)	Species
VSMC	Anti-α-actinin	AF 488	496/519	Mouse
	Anti-Troponin-I	AF 594	590/617	Rabbit
	SiR-actin	Cy5	650/670	Conjugated as is
CM	Anti-Paxillin	AF 488	496/519	Mouse
	Anti-SM actin	AF 594	590/617	Rabbit
	SiR-actin	Cy5	650/670	Conjugated as is

and intensity values, depending on the spot size and intensity. Nearest neighbour tracking is used for linking the detected spots to each other, by linking the closest spots between frames to each other. For tracking a minimum track length of 30 frames was used and a maximum of 2 missing frames.

1.4.4 Optical flow

The projection of an image creates a 2D path $\vec{x} \equiv \begin{bmatrix} x(t) \\ y(t) \end{bmatrix}$ with instantaneous velocities $\vec{v} = \frac{\mathrm{d}\vec{x}(t)}{\mathrm{d}t}$

The velocity for each point is called the 2D motion field. This motion field is what optical flow tries to estimate by using the intensity gradient over time and position. The basic principle of Optical flow is to estimate "brightness constancy", thus assuming the pixel intensity of whichever you track remain equal into the next frame.

$$I(\vec{x},t) = I(\vec{x}+\vec{v},t+1) \tag{1}$$

I represents the image intensity as a function of space and time. By assuming the moved image can be approximated by a first order Taylor series (the change must be small) it can be written like this.

$$I(\vec{x}+\vec{v},t+1) \approx I(\vec{x},t) + \vec{u} * \nabla I(\vec{x},t) + \frac{\mathrm{d}I(\vec{x},t)}{\mathrm{d}t} \tag{2}$$

Now enter equation (1) into the left part of equation (2) and we get.

$$\vec{u} * \nabla I(\vec{x},t) + \frac{\mathrm{d}I(\vec{x},t)}{\mathrm{d}t} = 0 \tag{3}$$

Which relates the spatial and the temporal derivatives directly to the velocity. This equation is called the "Gradient constraint equation". This only represents one equation whilst 2 are needed to determine u_1 and u_2. A method of further constraining u is to use the gradient constraints from neighbouring pixels.

Generally, no single velocity will satisfy all pixels, so a least-squares error estimator is calculated.

$$\sum_{\vec{x}} W[\vec{u} * \nabla I(\vec{x},t) + \frac{\mathrm{d}I(\vec{x},t)}{\mathrm{d}t}]^2 \tag{4}$$

W being a weight function, often Gaussian to give more weight to the neighbouring velocities than to those further from the relevant pixel. Though this is only the simplest of the many ways to add constraints to $\vec{u}$ The need for such an additional constraint is called the Aperture problem of optical flow algorithms[Fortun et al., 2015, Fleet and Wiess, 2006].

The above principle is the foundation for optical flow modelling though in the past 34 years many deviations and different algorithms have been developed. Optical flow modelling of the contraction images was performed using the ImageJ plugin Optic Flow. This plugin performs the Lucas-Kanade optical flow algorithm and accepts a gaussian sigma value, for which 4 was used.

1.5 Matlab Code

All the Matlab code for the analysis was written by the author and can be found under supplementary information.

1.5.1 Particle tracking code

The results from the particle tracking using the SOS ImageJ plugin are saved in several text files. The text file *tracks.simple.txt* contains the x and y coordinates for each track, track number, a logical value whether the track was active at that timeframe and the intensity and standard deviation of the fitted PSF. The file *tracks.simple.filtered.txt* removes the part of the tracks where the particle is inactive. It may be shown as immobile due to the plugin not picking up the movements due to large jumps between frame, inability to be detected using the specific size kernel or other mainly settings dependent defects. From the *tracks.simple.filtered.txt* Matlab imports the columns containing the X and Y coordinates and the first frame with detected movement. From *results.track.length.txt* the length of each track is extracted. This data is used to create a cell array with each cell containing a full track. To be able to make calculations with the tracks, the tracks missing values for certain frames (for the recorded data between 20-60% of the tracks spanned the whole video length) are supplemented with *NaN* values. From these coordinates vectors are calculated by taking the difference between each frame and another cell array is created where the cartesian vectors have been converted to Cartesian. To check the spread of the particles the first coordinate of each track is scatter plotted, and based upon the location of the first coordinate in 1 of 16 sections (4 along the x axis and 4 along the y axis) the tracks are placed into sections, by creating another cell array containing 16 cells.

After these preliminary steps, the radii are summed over all tracks and plotted over time to give a picture of the contractions. To add directionality to the image the dot product

$x_1 * x_2 + y_1 * y_2$ with an arbitrary vector $\langle\sqrt{2}/2, \sqrt{2}/2\rangle^T$ (unit length) is calculated. The dot product is highest when both vectors point in the same direction, 0 when the vectors are perpendicular and lowest when the vectors point in exactly opposite directions. Irrespective of the direction of the beating, this ensures that contraction and relaxation are shown in opposite directions, evaluation of the video is still necessary to determine which is the contraction and which relaxation.

The period was calculated by using an autocorrelation function. Finding the peaks and the average time difference between these the period can be calculated quite accurately. For series such as the one dealing with here, with multiple peak. It can be useful to specify a minimum peak prominence and height (based on the maximum value of the series for instance) to minimize the chance of calculating an incorrect value. In practice, it is advisable to check the plot and the period calculated.

For the whole set of tracks as well as per section the average direction is calculated by taking the circular mean

$$\vec{\alpha} = atan2 \sum_{j=1}^{n} sin(\alpha_j), \sum_{j=1}^{n} cos(\alpha_j)$$

To check for the homogeneity in each section, the same direction was considered as being within the same quadrant percent as the reference direction. In this case the mean angle was used as the reference. To calculate the percentage of tracks in a cell going the same direction, a polar histogram was created for the tracks in a section. The number of vectors in the same bin as the mean angle, was divided by the total number of vectors in the section.

This percentage can be plotted over time for each section (currently commented in the code, fig.23), but to ensure easy readability the weighted average was calculated (weighed by the number of tracks per section).

Finally, some statistics are calculated such as the standard deviation of the calculated period and the Pearson correlation coefficients between the homogeneity of the contractions and the contractions themselves.

1.5.2 Optical flow code

For the optical flow analysis, the performed analysis is practically identical while the execution was quite different. The Optical flow ImageJ plugin provides the data in the form of images. A 2-channel image is created of videolength-1 frames. These images contain the radii and the angle for the vectors of each pixel. When movement isn't detected, the image contains a *NaN* value. These images can be imported into Matlab and analysed in a similar fashion the particle tracks. For the optical flow analysis, another representation was created. By taking the angle for each section and playing this as a quiver plot in a video over time. Which allow for an easier overview, by only looking at 16 arrows and can be used to show a general direction as well as give a sense of homogeneity of the beating.

2. Results

2.1 Fixed cell microscopy

2.1.1 Smooth muscle cells

For the smooth muscle cell experiments, the Fibulin-4 mouse model was used. Cells were taken and cultured from the arch of the aorta of 3 different specimen. The wildtype (++), the R+ type, which is heterozygous for the fibulin-4 reduced expression allele and the RR type, homozygous for the fib-4 reduced expression allele, expressing approximately 4 times less fibulin-4 citefib4. Fibulins form connections between extracellular matrix structures in order to stabilise and organise the matrix. Underexpression can cause disorganisation of the extracellular matrix as well as the cellular cytoskeleton [Hanada et al., 2007, Ramnath et al., 2015].

Actin, Dapi, Smooth muscle actin and paxillin were stained. Paxillin is part of the focal adhesions, protein complexes that adhere to the ECM for force and signal transduction. In fig. 12 the results from the immunostaining can be seen. The wildtype shows homogeneous coverage of ample actin bundles and ordinary focal adhesions mainly visible at the ends of actin bundles. The R+ type displays less actin while the focal adhesions are generally as expected. The RR type presents little actin organisation, few bundles spanning the cell are present mostly showing on the edges of the cells. The focal adhesions of the RR type are present in the extremities of the cell, accumulating there in large amounts.

The lack of actin bundles due to disregulation of the cytoskeleton seen in the reduced fibulin-4 cells, likely result in the accumulation of paxillin in places where actin barbed ends are still present. The ++ images reveal the difference between smooth muscle and striated muscle especially well. The actin bundles show no bands in the filament intensity. In striated muscle bands would be expected.

In the future α-actinin can be stained in VSMCs due to the presence of the protein in dense bodies, which attach actin bundles to the cell membrane. This can be used for more accurate determination of a muscle structure in smooth muscle cells [Geeves et al., 2005].

2.1.2 Cardiomyocytes

Cardiomyocytes provided by Pluriomics were studied 9 days post-seeding. Cells used were healthy, mature, beating cells.

Cells studied had formed several clumps, connected by stretched cells. Figure 13 shows the tissue formations.

A monolayer of uniformly distributed cells is preferable for *in vivo* analysis, but poses no problem for confocal microscopy of internal muscle structures and the uniform beating behaviour indicates proper gap junction function between all cells, which are necessary for synchronous beating.

Multi-cell layers The cells were stained to visualise certain components of sarcomeres. Actin, α-actinin and Troponin. The expectation for striated muscle cells is to see band patterns in all 3 of these components, but at different intervals and positions. For increased clarity actin has been colored both yellow and magenta. As discussed in the introduction,

Figure 12. Paxillin in green, Smooth muscle actin in magenta, SiR-actin in red and DAPI in blue
A: Wild type (++), B: Heterozygous reduced fibulin-4 (R+), C: Homozygous reduced fibulin-4 (RR)

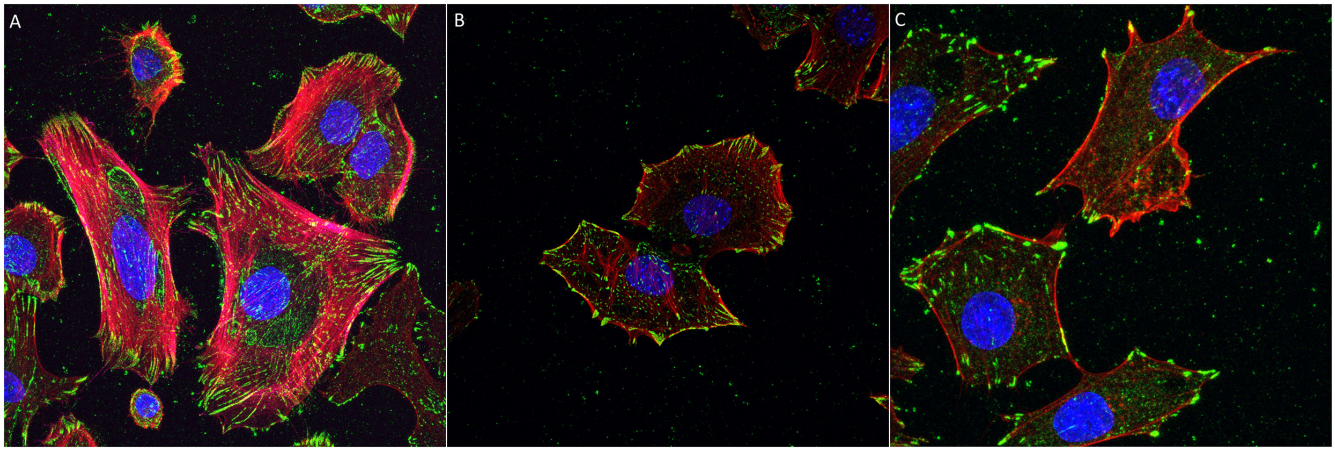

Figure 13. 3D cell structures formed after seeding

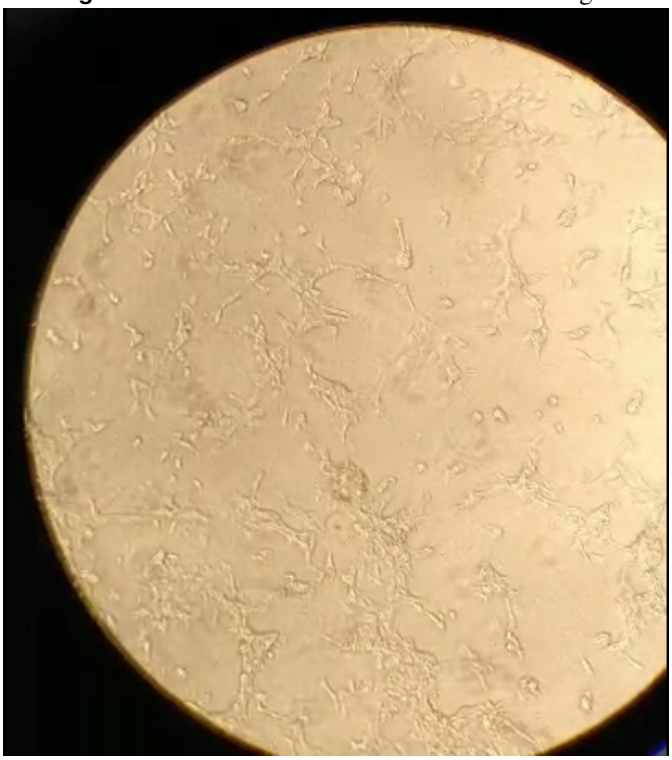

sarcomeres run from z-disk to z-disk, such that one sarcomere is demarcated by 2 actinin bands. In between these bands actin should be visible with the exception of a darker gap in the middle, where only myosin would be. Troponin should be present mainly on actin.

Proper staining of actin using the SiR-actin stain, could be promising for live cells staining of cardiomyocytes. If functional, sarcomere contraction would be visible as shortening and extension of the dark gap in the actin pattern.

In figure 14 A alls these components are overlaid with actin in yellow, the different fluorophores show alternation in intensity.

Figure 14 B shows the overlay of α-actinin (green) and troponin(red). Figure 14 E&F show the individual proteins. The thin actinin band falls into every second dark band of the troponin stain.
In figure 14 D actin (yellow) and troponin are compared. No troponin is present in the middle of the high intensity band of the actin pattern.
Finally, figure 14 G compares the actin and the α-actinin signals, α-actinin falls in the middle of the light actin band.

The immunofluorescence data suggests a functional contractile apparatus of the cells, with proteins present where expected. These cells should be suitable to perform experiments, since the control shows regular cardiomyocyte function.

The observation that light actin bands span 2 light troponin bands evoked discussion, whether the actin shouldn't show dark bands where the actinin binds 2 separate sarcomeres. Further research yielded no known actinin staining by SiR-actin, and looking at proposed actin-α-actinin binding schemes seems to support the finding that there is no darker band present on the actinin band[Panasenko and Gusev, 2000].

The clear visibility of striae on the actin bundles shows promise for live-cell staining using SiR-actin. SiR-actin is non-toxic and seems capable of visualising the sarcomeres by itself. If the actin remains stained for long enough, this could be tracked for a long period of time. Cardiomegaly is caused by filament slippage, which occurs and increases in severity over time. This could be used for tracking heart failure progression.

Isolated cell Images were taken of a single muscle cell without cell contact. No single cells were found to show any beating. Based upon literature there is no reason for single cells not to exhibit beating behaviour [Beussman et al., 2016]. The findings seemed to indicate this nonetheless, though no significance could be shown due to lack of a controlled environment for single cell maturation.

Figure 15 shows the internal structure of the single cells were disorganised. Very few sarcomeres are able to be dis-

Figure 14. Figure showing different overlays of stained F-Actin, Troponin-I, α-Actinin and DAPI. Ordered to simplify comparison of each stain.
A: Overlay of F-Actin(yellow), Troponin-I(Red), α-Actinin(Green) and DAPI(blue); B:Troponin-I, α-Actinin and DAPI; C: F-Actin(yellow); D: Overlay of F-Actin(yellow), Troponin-I and DAPI; E: Troponin-I; F: F-Actin(magenta); G: Overlay of F-Actin(magenta), α-Actinin and DAPI; H: α-Actinin

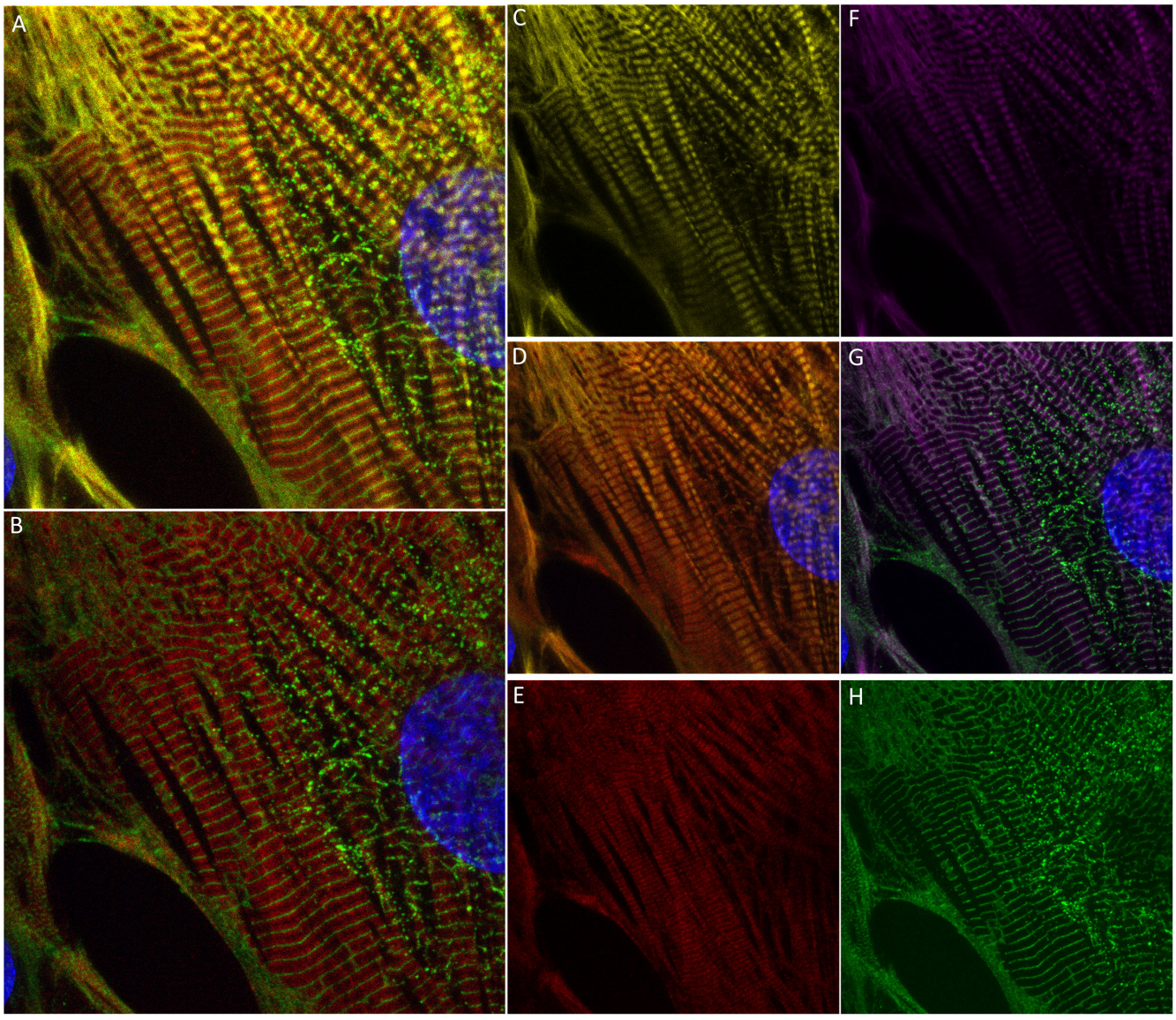

Figure 15. A single CM not touching any cells, nor beating. DAPI blue, Actin magenta, Troponin-I red and α-actinin green

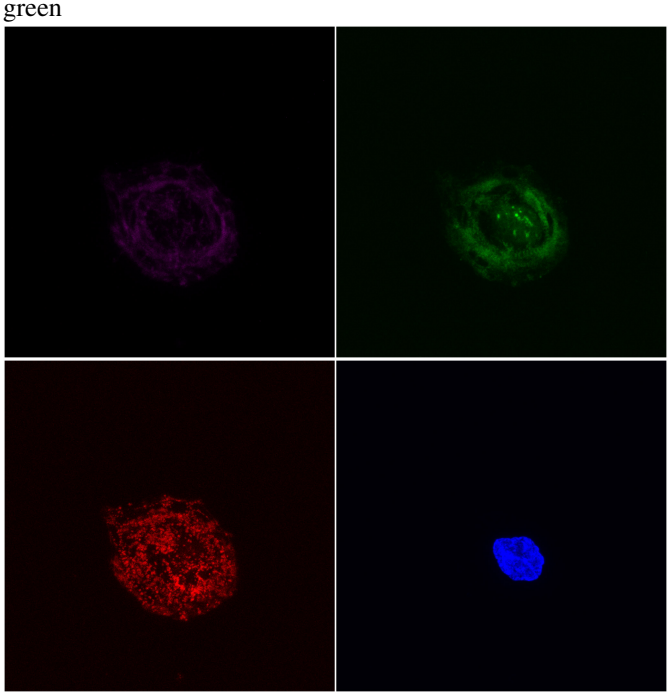

tinguished. Mainly the actinin seems to show some band patterns, mostly on the right side of the cell.

The image seems to explain that the cell wasn't beating, but it remains unclear why the muscle structures in these cells hadn't developed properly.

2.2 Image analysis Cardiomyocytes

2.2.1 Contraction plots

Optical flow Optical flow data creates outputs a 2D motion field between each 2 frames of the video. The motion field can be interpreted as the path travelled between separate frames. To extrapolate the period and beating pattern from the video, for each time point (one time point represents the path between 2 subsequent frames) the radii of the vectors are summed. In figure 16A (top) and B(top) the results of this summation are plotted. When more pixels move and the pixels move further, the peaks get higher and this results in a reasonable representation of the beating. Contraction and relaxation are both shown as positive movement, because there is no sense of direction associated with this plot. This plot therefore only gives a scalar value to the amount of movement occurring between each frame. But it can also be used to determine the relative coordination of beating, if the beating were happening out of sync, the peaks would be much wider and lower.

This analysis already proved to give an interesting result. On the 15 kPa contraction there is a small nudge in the peak. Upon closer inspection of the video there is a small hesitation in the contraction before the actual contracting. In the 100 kPa plot a much larger nudge is detected, characterised by a very high peak which quickly falls again. In this case in the video the hesitation is more easily spotted.

One way of adding a direction to this is to take the dot product between the vector at each point and an arbitrarily chosen vector. In this case the chosen vector had radius 1 and angle 45 degrees. This dot product was calculated separately for each pixel at each time point. Now the data can be plotted again with a direction added.

Which sign designates contraction or relaxation depends on the vector chosen. In the Ibidi data the vector resulted in contractions being shown as a negative peak.

The nudges in the 15 kPa plot are recognised as a small peak before the large negative peak for the contraction. The small hesitation seen at the beginning of the contraction is enough to tilt the movement to positive for a small moment before the full contraction.

The 100 kPa video shows a much more complex beating pattern, not only is the hesitation much larger, there seems to be one in the contraction and the relaxation. The first hesitation happens slightly later into the contraction than in the 15 kPa case, causing a much smaller negative peak. The second hesitation shows up very clearly, showing a positive and a negative peak in quick succession.

Currently, a possible explanation for this is the high stiffness of the PDMS these cells were grown on, requiring more force to move this might result in a less controlled beating. Possibly the PDMS requires more force to move than the cells are able to produce, and the bond between actin and myosin gets ruptured.[Geeves et al., 2005, Stewart et al., 2013]

Particle tracking With the particle tracking data, nearly the same approach was used. In this case using the coordinates for each frame, to calculate the path travelled between frames. An inherent difference between the particle tracking and the Optic flow is the data containing about 3 orders of magnitude less data points. Between 2000 and 10000 tracks were detected generally. While there are $2048 * 2048 = 4194304$ pixels for each frame. It is likely there were spots detected that were actually noise. Finally the paths calculated between frames can be directly linked to form a track. In the optical flow case, each motion vector is calculated between 2 frames. Tracing paths from this would require some sort of reference point, as well as sophisticated coding.

First thing obvious from the particle track data (fig. 16 C/D) is the stochasticity. The nudge in the peaks are barely visible, the times where there is zero movement in the optical flow (due to averaging), there is some movement detected.

An advantage to the particle tracking is the fact that there is little uncertainty about the data, the motion detected is likelier to be truthful. Optical flow uses the intensity gradients to determine motion, but some object change intensity during the video. Another issue this brings is the inability to recognise finer movements not in the general direction of motion, when neighbouring pixels all possess similar intensities (which is often the case). Optical flow models the motion while particle tracking attempts to measure it.

The most important advantage to the particle tracking is

that the actual deformation of the PDMS is measured. In the transmission light images, it is difficult to see if there is a true monolayer and if the PDMS is deformed by the same amount as the cell motion. Using the PDMS deformation from the fluorescent beads in combination with the elastic modulus this can be used to calculate the force exerted on the PDMS. Allowing the quantification of contractile forces by different cardiomyocyte cell lines, each with their own properties such as different pathologies induced by mutations.

Finally, a necessary approach for using the particle tracking data further is using a frame in between relaxation and subsequent contraction as a reference frame and subtracting this frame from each frame. This gives the position vector relative to the resting position for each frame, instead of the velocity vector, given by calculating the difference of neighbouring frames. If sufficiently accurate, this allows for absolution force calculation from PDMS deformation, without the requirement of a permanent anchoring point.

2.2.2 Period calculation

When looking at the periods calculated using the Optical flow methods in contrast to the Particle tracking method, a difference of respectively 6.2% and 53.2% is found with respect to the optical flow period. Despite the smaller difference in the 15 kPa case, both cases exhibit a significant ($p<0.001$) difference between calculated periods.

Upon closer visual inspection of the footage it became clear that this was no error in the calculation, but rather the images taken at a different time clearly exhibit slower beating.

Some explanations to be considered are: (1) The transmission and fluorescent images, though highly unlikely, might not have been recorded on the same sample, thus the beating rates are inherently different without a sine node directing the contraction. (2) The recording speed and time were not equal. If the camera was set to record 120 frames, but the frames per second were different. For instance, if the fluorescent image was recorded at 24 fps and the transmission light at 16 fps, the period for the transmission light should be $1.306\,s * \frac{24fps}{16fps} \approx 2\,s$. This would imply that the recording time for the transmission light was 7.5 seconds, which could be missed by the microscope operator, considering writing the data takes longer than recording it anyhow.

The issue with this explanation is that the 15 kPa recordings barely differ in period, so this could not explain that. Although the microscope settings might have been changed after the 15 kPa recording. (3) The beating rate changed between the different recordings, due to time or some external perturbation. Possibly it is a combination of these explanations, but there is no need to discredit the calculations due to the difference. Producing a vast amount more data is the solution and will also give a better idea of the usefulness of the analyses.

2.2.3 Directionality

Except for the coordination in time, there is also coordination in space which can be studied. How many cells move in the same direction? What is the average direction? Is there more coordination in contraction than in relaxation?

Since the cell borders are not visible, automated identification of individual cardiomyocytes is not possible using segmentation software. This restriction called for another approach to getting a more detailed picture of the movements of the beats. The images were sectioned based on position, using a 6x6 grid. Each of these 36 sections were used to separately calculate the average direction for each frame.

Figure 18 shows the 15 kPa transmission light video overlaid with a quiver plot, which depicts the magnitude and direction of the average motion for each of the sections.

Though a nice visual representation, there is no data to be formally extracted. It can be used as an aid for empirically checking numerical results.

For determining the amount of spatial coordination within a connected monolayer. It was attempted to think of a 'homogeneity'-measure for the directions. This was calculated by dividing the direction into the 4 wind-directions, considering an angle in the same quadrant as the same direction. For each section, the average angle was calculated and this was placed into a quadrant. However many pixels or spots fell in the same quadrant as the average angle, was used to calculate a percentage. This percentage, according to the author, gives a reasonable measure of the amount of cells beating in the overall direction.

To keep the data clear and not present 16 plots for 16 sections (fig.23), these percentages were averaged, weighed by the number of tracks in each section or non-*NaN* values in each section. The results are a periodic signal with percentages ranging mostly between 0% and +-75%.

Because of the periodicity it seemed sensible to overlay the percentage plot with the displacement plot. In figure 19, the dot product results' absolute values are overlaid with the homogeneity plot. The dot product is used because of the higher amount of information contained in it, and recognition of the contraction/relaxation. While the absolute value is used to depict the arbitrariness of the sign.

From the plots (fig. 19) there is a correlation between the percentage and the dot product. Indicating a coordinated contraction and relaxation, both movements garner percentages of above 60% coordination. This is particularly surprising, because there certainly seemed to be a more established direction upon contraction. Another noticeable property is the close agreement between the movements of the spots and the homogeneity in the particle tracking cases (fig. 19 B&D). This can also be seen in the Pearson's correlation coefficients. Which were 0.61 ($p < 10^{-12}$) and 0.88 ($p < 10^{-38}$) respectively for 15 kPa and 100 kPa.

Looking at figure 20 the homogeneity is compared when calculated as average from sections or from the whole image. In every case there is an increase in percentage when looking at the weighed percentages, which is expected considering the movement of the cells is not uniform, but within sections this is more likely.

In the optical flow cases there is a clear increase in peri-

Figure 16. Different displacement plots generated using optical flow and particle tracking data

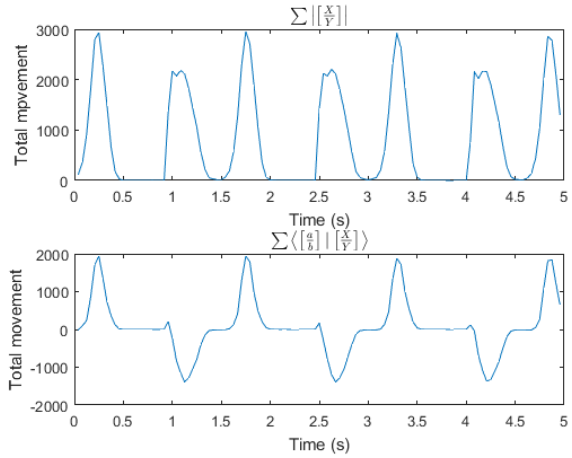

(a) 15 kPa Ibidi, optical flow displacement

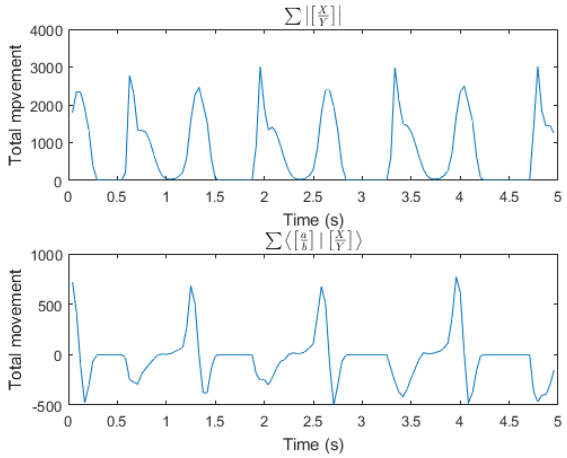

(b) 100 kPa Ibidi, optical flow displacement

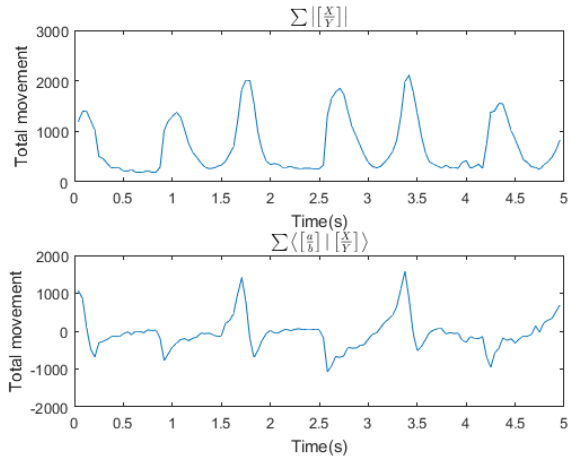

(c) 15 kPa Ibidi, particle tracking displacement

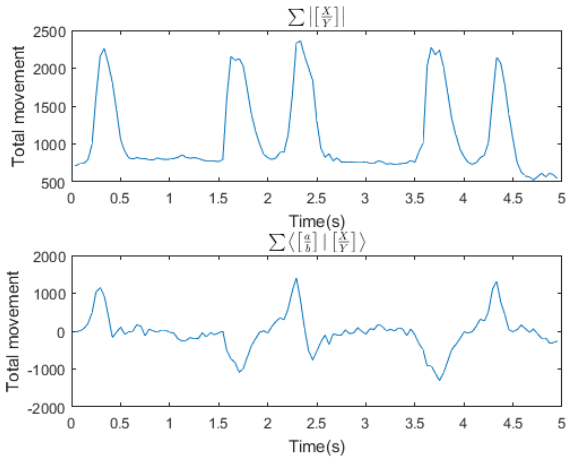

(d) 100 kPa Ibidi, particle tracking displacement

odicity of the homogeneity of the pixels. When no sections are used there is very little periodicity to be seen, while in the particle tracking case this is already clearly seen even when the whole image is analysed.

2.3 Image analysis VSMC

Smooth muscle cells were made to contract by supplementing the medium with 120 mM Potassium Chloride. Inducing contractions in the cells and filming these, attempts could be made to investigate the usefulness of the devised methods.

For this purpose, the matlab code had to be slightly adapted, mainly removing parts that were unnecessary for single contractions and parts that would require too much adaptation.

Previously 60 mM had been reported to induce contractions [Yeung et al., 2017, Waugh, 1962]. In these findings concentrations of 120 mM or above (180, 240 mM) induced contraction without shrinking the cells due to hyper-osmolarity of the extracellular fluid.

A limited number of cells were contractive, most cells were likely in different, non-contractile, stages of differentiation. [Rensen et al., 2007]

In figure 21 the first and last frame of one of the recordings are shown, the cell roughly in the middle clearly shows contraction of the extremities and compaction of the main body of the cell.

Optical flow was also performed (fig. 21) on the VSMC footage. The results are very noisy, but the contraction can be clearly seen. Seeing an increase of approximately 23% over the background, which is higher than expected considering there was only a single cell contracting. The background was mainly caused by turbulent flow caused by adding the KCl solution too abruptly.

In the live cell VSMC experiments, SiR-actin has been added to several plates. In figure 22 the result of one of these is shown. This result seems to indicate that SiR-actin is not toxic for VSMCs, for at least relatively short periods of time.

Figure 17. Comparing the calculated periods using Optic flow or particle tracking

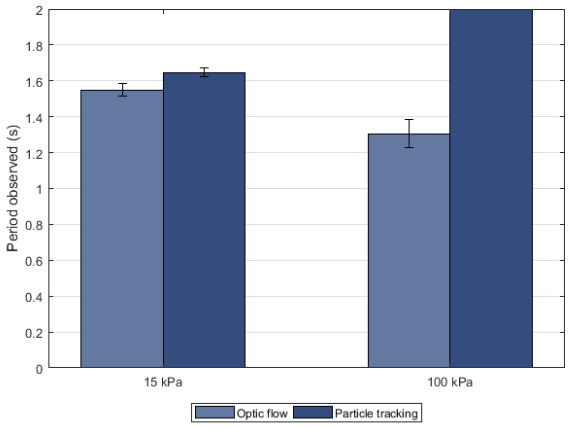

Using a larger sample size and higher resolution camera would allow for detailed analysis of the actin, if this result can be repeated.

This plot shows there might be benefits garnered from using the method on different contractile cells. To study smooth muscle cell contraction in a non-destructive way that can be performed repeatedly and very fast, under many different conditions can be a useful addition to the toolbox of cardiovascular research.

3. Discussion

In the results obtained from the image analysis there are differences to be seen between the cells grown on different substrate flexibilities. This seems to indicate that the flexibility of the substrate matters in displacement distance. If more data has been gathered and this expectation is confirmed. One can move onto the next step, which is applying the assay to diseased cell models. Checking to see if these are properties that can be found in small scale cell culture. There are hundreds of genetic mutations to be examined in heart failure research. If this assay works, this would be a very good way to study the behaviour of cells in a non-destructive manner over a longer period of time.

Not only the displacement but also the coordination of the cells, governed by amongst other things, cell adhesion (through gap junctions) are important factors in healthy heart function. Using the proposed methods these can also be studied to a certain degree, especially when combined with for instance patch-clamp experiments for studying the conductance over larger cell layers.

Due to the duration of the project though, very little data has been acquired to support the interpretations made. The author was unable to produce stable, beating monolayers of cardiomyocytes with usable results. This means that before further research is performed the current methods need to be backed-up.

Figure 18. Frame 25 overlaid with quivers indicating the average direction of that

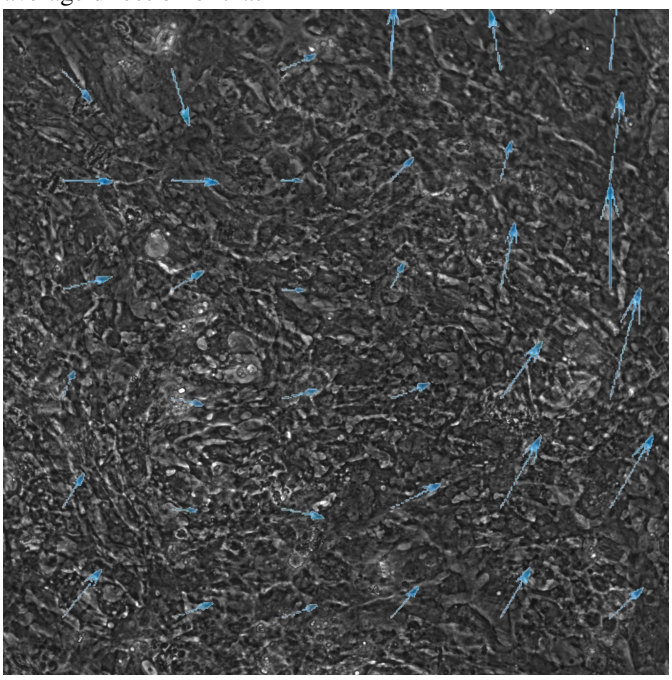

Issues with the optical flow analysis front, are that it doesn't create paths of objects, but treats each 2 subsequent frames as separate. Because of this, combined with the inherent properties of optical flow, constant motion is shown as a straight line (the speed of the object is essentially modelled). This doesn't make the technique unusable, but it is limiting in its usefulness. On top of this transmission images are risky to use, because of the lack of certainty that only a single layer of cells is contracting and if the PDMS is moving as much as the cells are. If this is not the case, the attached contraction-force value one might calculate, cannot be compared to other cultures.

For the particle tracking analyses, these could also be analysed in a different manner from the optical flow data, as mentioned in the results, by calculating position vectors as opposed to velocity vectors. This doesn't compare to the optical flow data, but adds information not gathered from the optical flow data because the particle tracking does represent paths.

Studying the behaviour of the internal muscle structures during contraction is also interesting. But live staining of actin structures, have been attempted once but have failed. The toxicity of actin has not been tested on the cardiomyocytes. Another thing is that SiR-actin is pumped out of the cells, to counteract this verapamil is used [Lukinavičius et al., 2014], but this would stop contraction due to blocking of calcium channels. Finally, the contractions might not be visible enough to allow data extraction at all.

Possibly, SiR-actin is not usable for live imaging of cardiomyocytes. In that case other methods should be found, for instance transfecting the cells with GFP-coupled α-actinin

Figure 19. Plots comparing the homogeneity of direction of pixels/tracks to movement

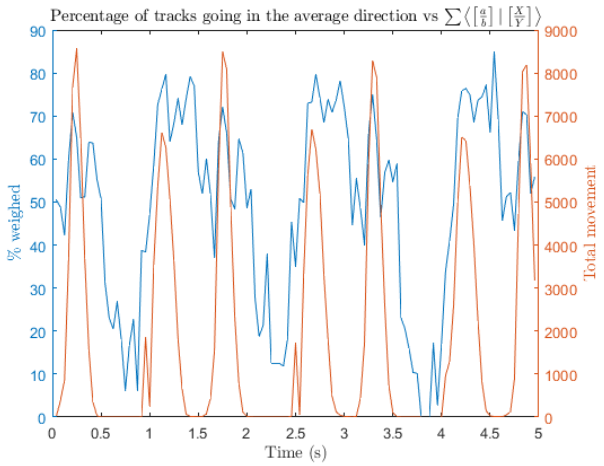

(a) 15 kPa Optic flow vs. %

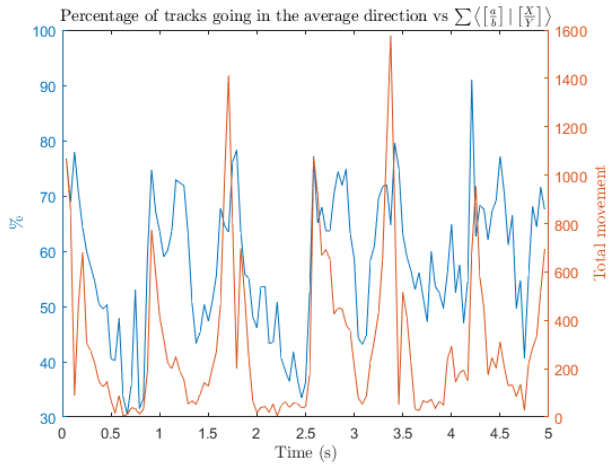

(b) 15 kPa Particle tracking vs. %

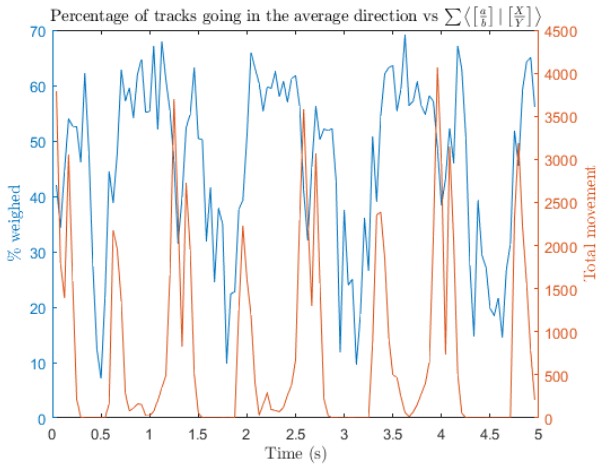

(c) 100 kPa Optic flow vs. %

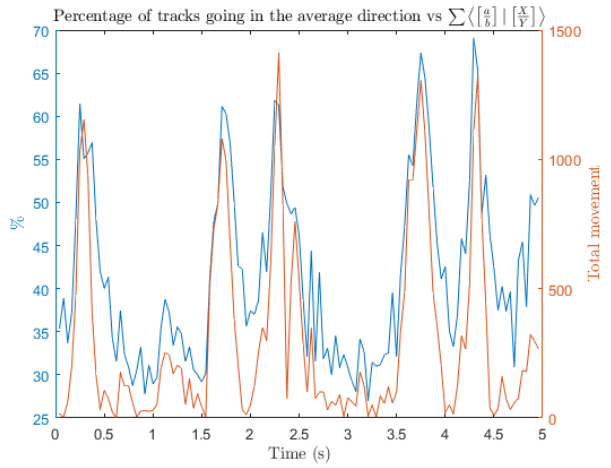

(d) 100 kPa Particle tracking vs. %

[Hersch et al., 2013].

There are different ways to expand on the techniques used in this paper. First, the micropole arrays mentioned in the introduction can provide a measurement of the contractile strength of single heart muscle cells. And filming single cells on flat PDMS surfaces can also be very useful for studying the compaction of single cells, this could be extrapolated to confluent cell layers to estimate the optimal total contraction. Single cell data is less representative of actual heart tissue, but does allow more accurate quantification of properties, which can be used when moving onto larger tissues.

Looking at the considerations, traction force microscopy is a technique similar to what has been done in this paper, but with some expansions. Like the fluorescent beads assay, but in traction force microscopy the beads are anchored at the bottom of the PDMS as well (sometimes with a different fluorescent label). This way there is a permanent anchoring point which can be used to couple a the resting position to the cells and track the deformation of the PDMS much more carefully. Which can subsequently be used to calculate the Greens tensor, which relates the deformation of a substrate to a point force. This is sensible because the force exerted on the PDMS mainly comes from discrete points that attach the sarcomeres to the membrane, the costameres. By staining vinculin for instance, these adhesions can be visualised as well [Hersch et al., 2013, Merkel et al., 2007]. A disadvantage of using fluorescence is the inability to record transmission light and fluorescent light images simultaneously. Because of the usefulness of the transmission light images, this would rather not be absent. And as seen in figures 16&17 different times of recording can lead to major differences. Possibly, combining optical imaging with magnetic imaging, using magnetic nanoparticles for markers, could be a solution for more accurate 3D tracking of the movements[Le Sage et al., 2013].

Finding ways to perform higher dimensional analyses on 3D tissue is an essential part of creating this model. And for

Figure 20. Plots comparing the homogeneity of direction when calculated per section or per image

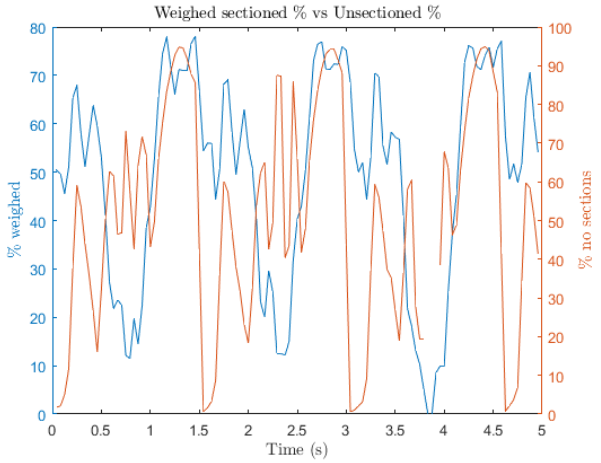

(a) 15 kPa Optic flow

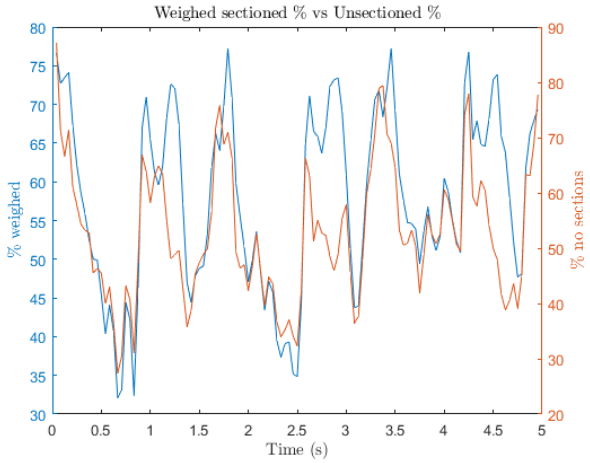

(b) 15 kPa Particle tracking

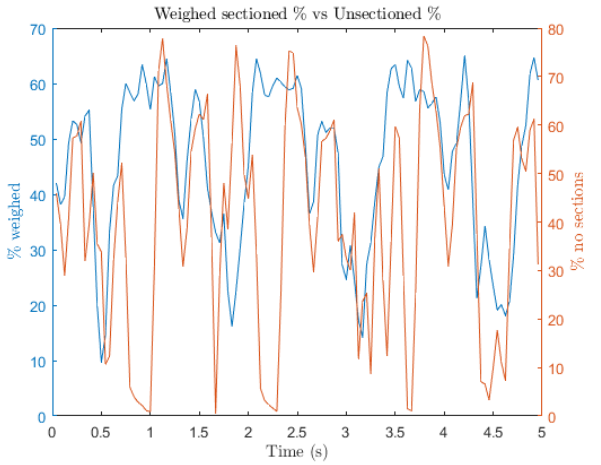

(c) 100 kPa Optic flow

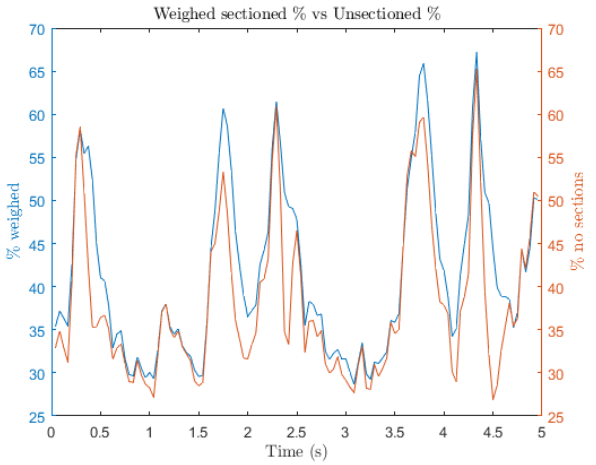

(d) 100 kPa Particle tracking

this method to be non-destructive would be a great benefit because studying the model for a long time is essential if it is going to be used for actual drug testing.

Acknowledgments

I gratefully acknowledge the support and generosity of Pluriomics and Ibidi GmbH for the provision of the cardiomyocytes respectively the PDMS substrate plates, without which the present study could not have been completed. More specifically I would like to thank Jeroen Essers for his ongoing support during my project. Erik Meijering for his support with the necessary image analysis. And finally, Eduardo Mendes, Kai Zhang and Benjamin Klemm from the department of Chemical Engineering for providing the PDMS micropoles, despite not being able to use these in the project.

Figure 21. First and last frame ($\Delta t \approx 12$ seconds) of the contraction of a vascular smooth muscle cell and optical flow analysis

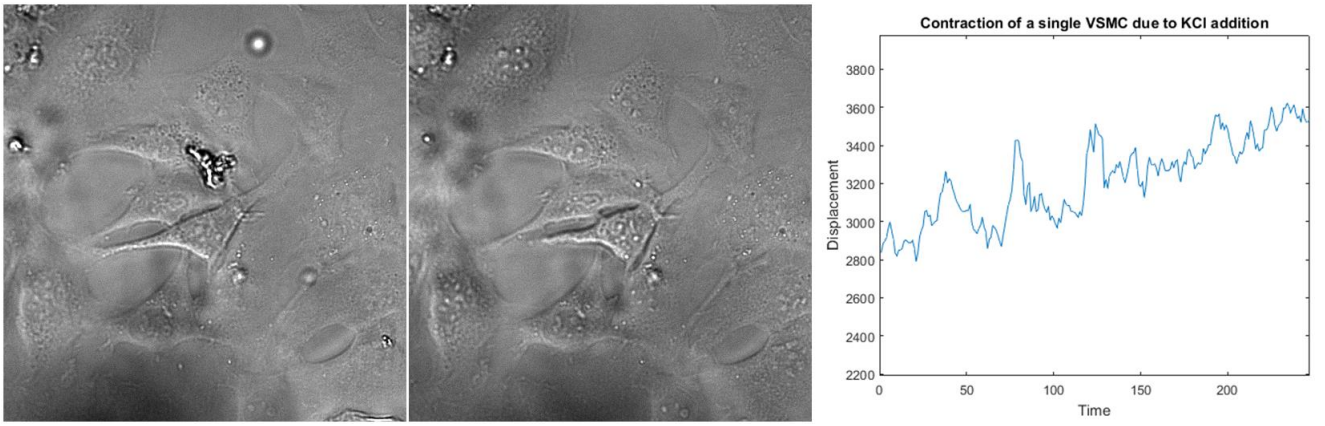

Figure 22. First and last frame ($\Delta t \approx 22$ seconds) of the contraction of actin in a VSMC

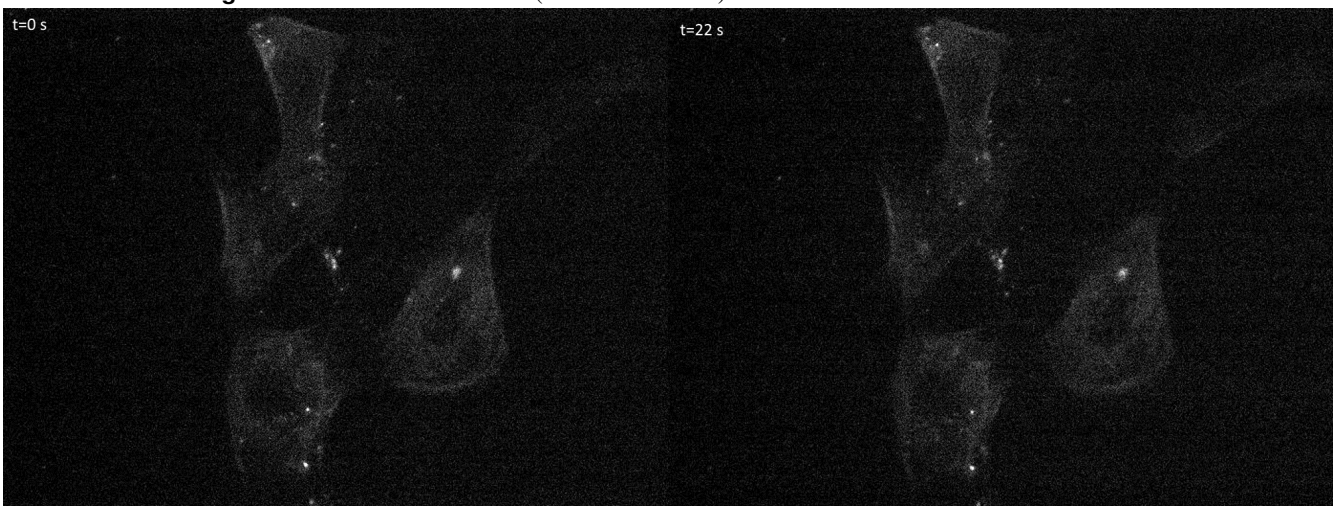

References

[Beussman et al., 2016] Beussman, K. M., Rodriguez, M. L., Leonard, A., Taparia, N., Thompson, C. R., and Sniadecki, N. J. (2016). Micropost arrays for measuring stem cell-derived cardiomyocyte contractility. *Methods*, 94:43–50.

[Brozovich et al., 2016] Brozovich, F. V., Nicholson, C., Degen, C., Gao, Y. Z., Aggarwal, M., and Morgan, K. G. (2016). Mechanisms of vascular smooth muscle contraction and the basis for pharmacologic treatment of smooth muscle disorders. *Pharmacological reviews*, 68(2):476–532.

[CDC, 2015] CDC (2015). https://www.cdc.gov/heartdisease/facts.htm.

[Chown and Kumar, 2007] Chown, M. G. and Kumar, S. (2007). Imaging and manipulating the structural machinery of living cells on the micro-and nanoscale. *International journal of nanomedicine*, 2(3):333.

[Commons, 2007] Commons, W. (2007). Haemocytometer grid. File:Haemocytometer Grid.png.

[Den Hartogh and Passier, 2016] Den Hartogh, S. C. and Passier, R. (2016). Concise review: fluorescent reporters in human pluripotent stem cells: contributions to cardiac differentiation and their applications in cardiac disease and toxicity. *Stem Cells*, 34(1):13–26.

[Fleet and Wiess, 2006] Fleet, D. and Wiess, Y. (2006). *Optical Flow Estimation, Handbook of Mathematical Models in Computer Vision.* Springer.

[Fortun et al., 2015] Fortun, D., Bouthemy, P., and Kervrann, C. (2015). Optical flow modeling and computation: a survey. *Computer Vision and Image Understanding*, 134:1–21.

[Geeves et al., 2005] Geeves, M. A., Fedorov, R., and Manstein, D. J. (2005). Molecular mechanism of actomyosin-based motility. *Cellular and Molecular Life Sciences*, 62(13):1462–1477.

[Gutierrez and Groisman, 2011] Gutierrez, E. and Groisman, A. (2011). Measurements of elastic moduli of silicone gel substrates with a microfluidic device. *PLoS One*, 6(9):e25534.

[Hall and Guyton, 2016] Hall, J. E. and Guyton, A. C. (2016). *Guyton and Hall textbook of medical physiology*. Elsevier.

[Hanada et al., 2007] Hanada, K., Vermeij, M., Garinis, G. A., de Waard, M. C., Kunen, M. G., Myers, L., Maas, A., Duncker, D. J., Meijers, C., Dietz, H. C., Kanaar, R., and Essers, J. (2007). Perturbations of vascular homeostasis and aortic valve abnormalities in fibulin-4 deficient mice. *Circulation Research*, 100(5):738–746.

[Heartchip, 2015] Heartchip (2015). *E - HeartCHIP: A novel in vitro organ-on-a-chip heart failure model for drug development*.

[Hersch et al., 2013] Hersch, N., Wolters, B., Dreissen, G., Springer, R., Kirchgeßner, N., Merkel, R., and Hoffmann, B. (2013). The constant beat: cardiomyocytes adapt their forces by equal contraction upon environmental stiffening. *Biology open*, page BIO20133830.

[Ibrahim et al., 2011] Ibrahim, M., Gorelik, J., Yacoub, M. H., and Terracciano, C. M. (2011). The structure and function of cardiac t-tubules in health and disease. *Proceedings of the Royal Society of London B: Biological Sciences*, 278(1719):2714–2723.

[Kim et al., 2015] Kim, J. J., Yang, L., Lin, B., Zhu, X., Sun, B., Kaplan, A. D., Bett, G. C., Rasmusson, R. L., London, B., and Salama, G. (2015). Mechanism of automaticity in cardiomyocytes derived from human induced pluripotent stem cells. *Journal of molecular and cellular cardiology*, 81:81–93.

[Krans, 2010] Krans, J. (2010). The sliding filament theory of muscle contraction. *Nature Education*, 3(9):66.

[Le Sage et al., 2013] Le Sage, D., Arai, K., Glenn, D., DeVience, S., Pham, L., Rahn-Lee, L., Lukin, M., Yacoby, A., Komeili, A., and Walsworth, R. (2013). Optical magnetic imaging of living cells. *Nature*, 496(7446):486–489.

[Lukinavičius et al., 2014] Lukinavičius, G., Reymond, L., D'este, E., Masharina, A., Göttfert, F., Ta, H., Güther, A., Fournier, M., Rizzo, S., Waldmann, H., et al. (2014). Fluorogenic probes for live-cell imaging of the cytoskeleton. *Nature methods*, 11(7):731–733.

[McDonagh et al., 2011] McDonagh, T. A., Gardner, R. S., Clark, A. L., and Dargie, H. (2011). *Oxford textbook of heart failure*. Oxford University Press.

[Merkel et al., 2007] Merkel, R., Kirchgeßner, N., Cesa, C. M., and Hoffmann, B. (2007). Cell force microscopy on elastic layers of finite thickness. *Biophysical journal*, 93(9):3314–3323.

[Özçam et al., 2014] Özçam, A. E., Efimenko, K., and Genzer, J. (2014). Effect of ultraviolet/ozone treatment on the surface and bulk properties of poly (dimethyl siloxane) and poly (vinylmethyl siloxane) networks. *Polymer*, 55(14):3107–3119.

[Panasenko and Gusev, 2000] Panasenko, O. O. and Gusev, N. B. (2000). Simultaneous interaction of actin with a-actinin and calponin. *IUBMB life*, 49(4):277–282.

[Pluriomics,] Pluriomics. Pluricyte®cardiomyocyte manual.

[Ramnath et al., 2015] Ramnath, N., Hawinkels, L., Van Heijningen, P., te Riet, L., Paauwe, M., Vermeij, M., Danser, A., Kanaar, R., ten Dijke, P., and Essers, J. (2015). Fibulin-4 deficiency increases tgf-β signalling in aortic smooth muscle cells due to elevated tgf-β2 levels. *Scientific reports*, 5.

[Rensen et al., 2007] Rensen, S. S., Doevendans, P. A., and van Eys, G. J. (2007). Regulation and characteristics of vascular smooth muscle cell phenotypic diversity. *Netherlands Heart Journal*, 15(3):100–108.

[Reuter et al., 2014] Reuter, M., Zelensky, A., Smal, I., Meijering, E., van Cappellen, W. A., de Gruiter, H. M., van Belle, G. J., van Royen, M. E., Houtsmuller, A. B., Essers, J., et al. (2014). Brca2 diffuses as oligomeric clusters with rad51 and changes mobility after dna damage in live cells. *J Cell Biol*, 207(5):599–613.

[Smal et al., 2012] Smal, I., Carranza-Herrezuelo, N., Klein, S., Wielopolski, P., Moelker, A., Springeling, T., Bernsen, M., Niessen, W., and Meijering, E. (2012). Reversible jump mcmc methods for fully automatic motion analysis in tagged mri. *Medical image analysis*, 16(1):301–324.

[Sniadecki and Chen, 2007] Sniadecki, N. J. and Chen, C. S. (2007). Microfabricated silicone elastomeric post arrays for measuring traction forces of adherent cells. *Methods in Cell Biology*, 83:313 – 328. Cell Mechanics.

[Somlyo and Somlyo, 1994] Somlyo, A. P. and Somlyo, A. V. (1994). Signal transduction and regulation in smooth muscle. *Nature*, 372(6503):231.

[Stewart et al., 2013] Stewart, T. J. et al. (2013). Actin sliding velocities are influenced by the driving forces of actin-myosin binding. *Cellular and molecular bioengineering*, 6(1):26.

[Waugh, 1962] Waugh, W. H. (1962). Role of calcium in contractile excitation of vascular smooth muscle by epinephrine and potassium. *Circulation research*, 11(6):927–940.

[Xu et al., 2007] Xu, Y., Hua, T.-C., Sun, D.-W., Zhou, G.-Y., and Xu, F. (2007). Effects of freezing rates and dimethyl sulfoxide concentrations on thermal expansion of rabbit aorta during freezing phase change as measured by thermo mechanical analysis. *Journal of biomechanics*, 40(14):3201–3206.

[Yeung et al., 2017] Yeung, K. K., Bogunovic, N., Keekstra, N., Beunders, A. A., Pals, J., Kuij, K., Overwater, E., Wisselink, W., Blankensteijn, J. D., Hinsbergh, V. W., et al. (2017). Transdifferentiation of human dermal fibroblasts to smooth muscle-like cells to study the effect of myh11 and acta2 mutations in aortic aneurysms. *Human mutation*, 38(4):439–450.

Supplementary information

See below for supplementary figures and the code written for the project.

Figure 23. Showing the spread of the detected particles for both the 15 kPa and the 100 kPa images provided by Ibidi

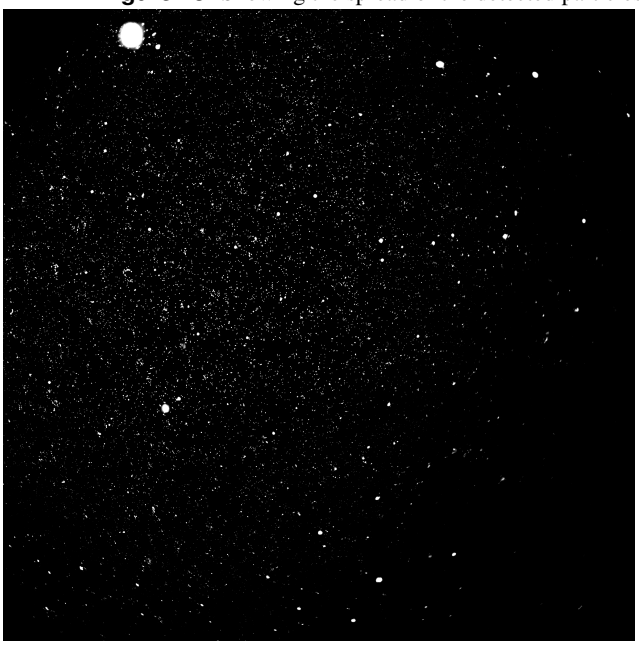

(a) First frame used for detection15 kPa

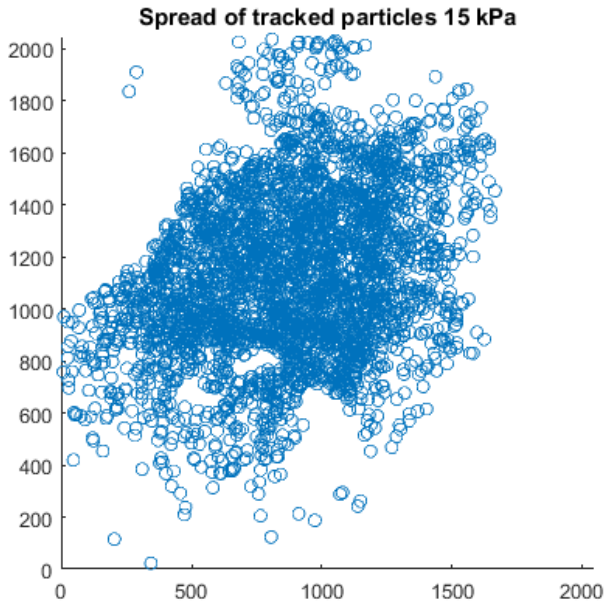

(b) First frame detected 15 kPa

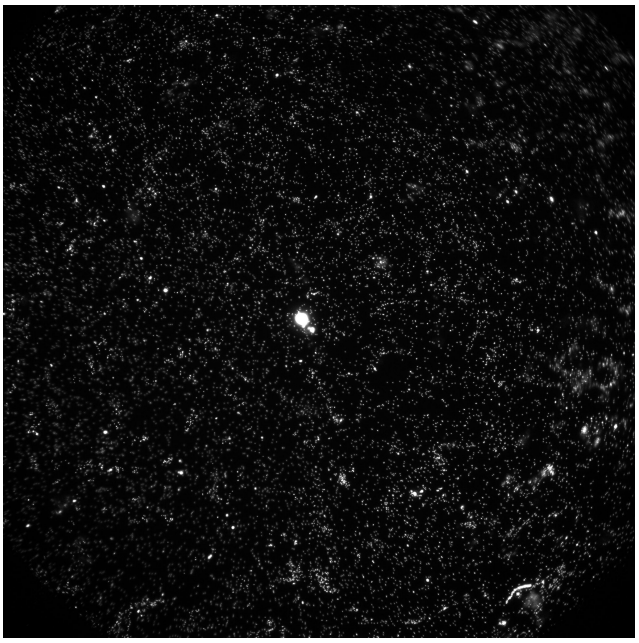

(c) First frame used for detection 100 kPa

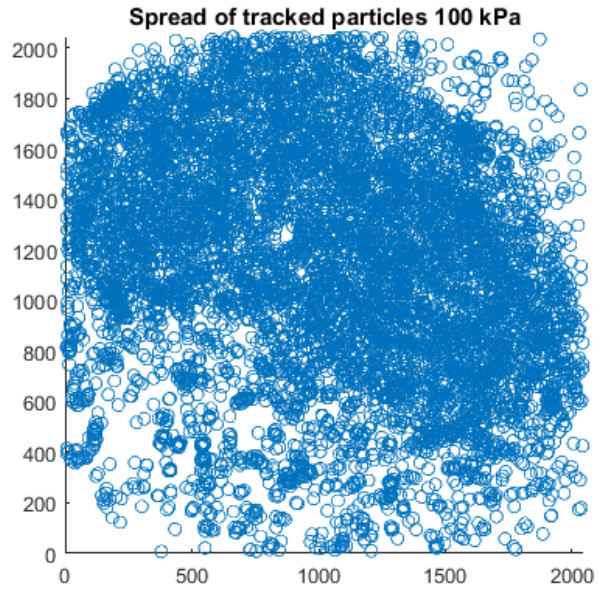

(d) First frame detected 100 kPa

Figure 24. Subplots example for 16 sections of 15 kPa optical flow data

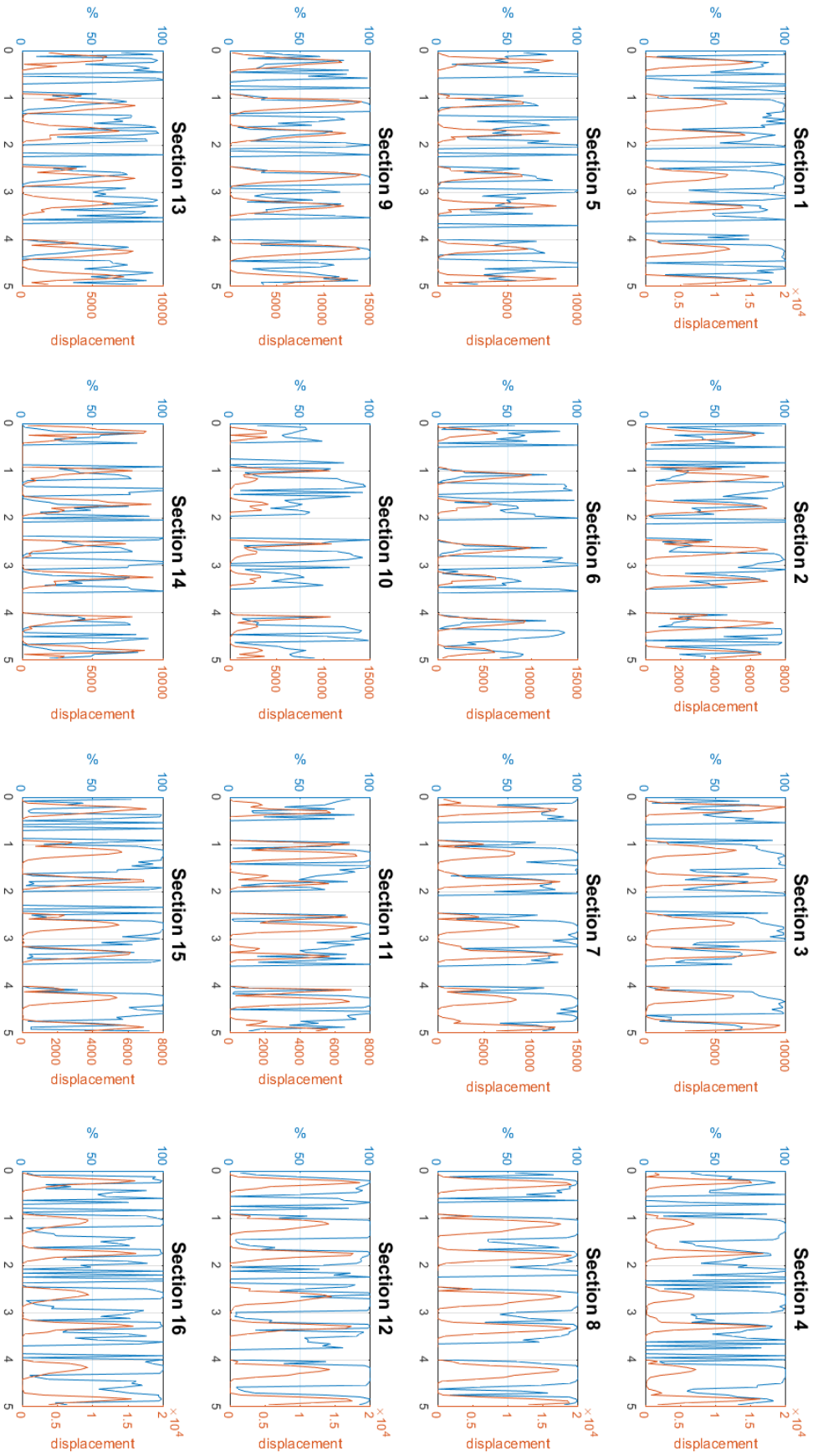

3.1 Matlab code

```
clearvars; close all;
cd('C:\BEP\MATLAB');
[filename, foldername] = uigetfile({'*.*'}, '
    Select File R');
if filename~=0
    r_file=fullfile(foldername, filename);
else
    quit
end
[filename2, foldername2] = uigetfile({'*.*'}, '
    Select File Phi');
if filename~=0
    phi_file=fullfile(foldername2, filename2);
end
prompt = {'X resolution','Y resolution','Number of
     frames','FPS','Shear modulus','Pixel size','
    Sections'};
dlg_title = 'Input';
num_lines = 1;
defaultans = {'2048','2048','119','24','15E3','
    0.33E-6','16'};
answer1 = inputdlg(prompt,dlg_title,num_lines,
    defaultans);
answer=str2double(answer1);
%% Read the tiff files and sum the displacement
tic
x_res=answer(1);
y_res=answer(2);
t_res=answer(3);
[r,phi,dX] = Tiff2mat(r_file,phi_file,x_res,y_res,
    t_res); %dX is in pixels
tee(1)=toc;
%% turn the polar matrices into cartesian
tic
[x,y]=pol2cart(phi,r);
tee(2)=toc;

%% Take improduct with arbitrary vector
tic
%dotproduct polar is (r1,?1)?(r2,?2)=r1r2cos
    (?1??2)
%dotproduct cartesian is x1*x2+y1*y2
% arb_vec(1,:)=[0;1];
% arb_vec(2,:)=[1;0];
arb_vec(1,:)=[sqrt(2)/2;sqrt(2)/2];%arbitrair
    gekozen vector 45 graden 1 lang
% arb_vec(4,:)=[1/2;sqrt(3)/2];
% arb_vec(5,:)=[sqrt(3)/2;1/2];
% for i=1:length(arb_vec)
[~,dIm(1,:)]=improduct(x,y,arb_vec(1,:),t_res,
    y_res,x_res);
% end
tee(3)=toc;
%% Calculate the force and the displacement when
    summed all together per time frame
tic
t=1:t_res;
fps=answer(4);
tijd=t./fps;
G=answer(5);
pix_size=answer(6);
pix_size_mm=pix_size*1000;
sectie=answer(7);
vak=sqrt(sectie);
A=pix_size^2;
v_c=10E-6; %inhoud gel
rhe=2E-3; %straal PDMS oppervlakte
l=v_c/(rhe^2*pi); %dikte PDMS
sumforce=(G*A/l).*dX; %force calculated from
    absolute displacement
tee(4)=toc;
%% Find period of beating by autocorrelation
tic
[autocor,lag]=xcorr(dIm); %crosscorrelate with
    itself
[~,lcsh] = findpeaks(autocor);
[pklg,lclg] = findpeaks(autocor,'MinPeakDistance',
    ceil(mean(diff(lcsh))),'MinPeakheight',0.6E11)
    ;
long = [mean(diff(lclg))/fps,std(diff(lclg))/fps];
subplot(2,1,1)
plot(lag,autocor)
grid minor
subplot(2,1,2)
plot(t,dIm)
grid minor
tee(5)=toc;
%% Plot force/displacement
tic
figure(1)
% h=animatedline;
subplot(2,1,1)
plot(tijd,dX*pix_size_mm)
axis([0 (t_res+1)/fps 0 1.2*max(dX)*pix_size_mm])
% H(t_res+1)=struct('cdata',[],'colormap',[]);
% H(1)=getframe(gcf);
% for k=1:length(tijd)
%     addpoints(h,tijd(k),S_F(k));
title('$\sum \left | \left [ \frac{X}{Y} \right ]
    \right |$','interpreter','latex')
xlabel('Time (s)')
ylabel('Displacement')
subplot(2,1,2)
plot(tijd,dIm*pix_size_mm)
legend('show')
axis([0 (t_res+1)/fps 1.2*min(min(dIm))*
    pix_size_mm 1.2*max(max(dIm))*pix_size_mm])
% H(t_res+1)=struct('cdata',[],'colormap',[]);
% H(1)=getframe(gcf);
% for k=1:length(tijd)
%     addpoints(h,tijd(k),S_F(k));
%title('$\sum \left \langle \left [ \frac{1/2\sqrt
    {2}}{1/2\sqrt{2}} \right ]|\left [ \frac{X}{Y}
     \right ] \right \rangle$','interpreter','
    latex')
title('$\sum \left \langle \left [ \frac{a}{b} \
    right ]|\left [ \frac{X}{Y} \right ] \right \
    rangle$','interpreter','latex')
xlabel('Time (s)')
ylabel('Displacement')
%annotation('textbox',[.3 .3 .3 .3],'String',
    sprintf('The frequency is %f Hz',round(
    Frequency,3)),'FitBoxToText','on');
legend('show')

%set ( ax, 'visible', 'off')
%     drawnow
%     H(k+1)=getframe(gcf);
% end
% w = VideoWriter('Ding_100kpa.avi');
% open(w)
% writeVideo(w,H)
% close(w)
tee(6)=toc;
%% Section the matrix into # regions
tic
warning('off','all')
sectiecellmean=cell(sectie,1);
```

```
x_sectie=sectionmean(x,sectie,t_res);
y_sectie=sectionmean(y,sectie,t_res);
tel=1;
for j=1:vak
    for i=1:vak
        a(:,1)=x_sectie(i,j,:);
        a(:,2)=y_sectie(i,j,:);
        sectiecellmean{tel}=a;
        tel=tel+1;
    end
end

sectiecellx=cell(sectie,1);
sectiecelly=cell(sectie,1);
tel=1;
aantal=length(x);
b=aantal/vak;
i3=0:(vak-1);
i2=1:vak;
for i=1:vak
    for j=1:vak
        A=x((i3(i)*b+1):i2(i)*b,(i3(j)*b+1):i2(j)*b,:);
        B=y((i3(i)*b+1):i2(i)*b,(i3(j)*b+1):i2(j)*b,:);
        sectiecellx{tel,1}=A;
        sectiecelly{tel,1}=B;
        tel=tel+1;
    end
end
tee(7)=toc;
%% Improduct with each section & Take the mean of the improducts of all the
[een, dImsec]=cellfun(@improductcell,sectiecellx,sectiecelly,'UniformOutput',0);
dIms=reshape(cell2mat(dImsec),[119 16]);
dImsmeans=mean(dIms,2);
%% Section the matrix with angles
sectiecellphi=cell(sectie,1);
tel=1;
aantal=length(phi);
b=aantal/vak;
i3=0:(vak-1);
i2=1:vak;
for i=1:vak
    for j=1:vak
        A=phi((i3(i)*b+1):i2(i)*b,(i3(j)*b+1):i2(j)*b,:);
        sectiecellphi{tel}=A;
        tel=tel+1;
    end
end
%% Histogram

clearvars cellplaats av_ang percgoed tid ph edges count ph2 count2 ind count2 ind totaal goed
cellplaats=cell(sectie,1);
av_ang=zeros(t_res,sectie);
percgoed=zeros(t_res,sectie);
bins=4;
edges=[-pi -pi/2 0 pi/2 pi];
for i=1:t_res
    tid=phi;
    ph=polarhistogram(tid(:,:,i),edges);
    count=ph.BinCounts;
    av_ang(i)=atan2(nansum(nansum(sin(tid(:,:,i))),nansum(nansum(cos(tid(:,:,i))))));
    ph2=polarhistogram(av_ang(i),edges);
    count2=ph2.BinCounts;
    ind=find(count2~=0);
    totaal=sum(count);
    goed=count(ind);
    percgoed_al(i)=(goed./totaal).*100;
    %         if isnan(tid)==1
    %             break
    %         end
end

%% Histograms per section
tic
clearvars cellplaats av_ang percgoed tid ph edges count ph2 count2 ind count2 ind totaal goed
cellplaats=cell(sectie,1);
av_ang=zeros(t_res,sectie);
percgoed=zeros(t_res,sectie);
bins=4;
%edges=[-pi -pi/2 0 pi/2 pi];
for j=1:sectie
    for i=1:t_res
        tid=sectiecellphi{j};
        ph=polarhistogram(tid(:,:,i),bins);
        edge=ph.BinEdges;
        count=ph.BinCounts;
        av_ang(i,j)=atan2(nansum(nansum(sin(tid(:,:,i)))),nansum(nansum(cos(tid(:,:,i)))));
        ph2=polarhistogram(av_ang(i,j),edge);
        count2=ph2.BinCounts;
        ind=find(count2~=0);
        totaal(i,j)=sum(count);
        goed(i,j)=count(ind);
        percgoed(i,j)=(goed(i,j)./totaal(i,j)).*100;
        %         if isnan(tid)==1
        %             break
        %         end
    end
end
percgoed(isnan(percgoed))=0;
mien=nanmean(percgoed,2);
tee(8)=toc;
%% Plot the average (of all sections) dotproduct result and the average percentage correct angles together
yyaxis left
plot(t',mien)
ylabel('%')
yyaxis right
plot(t',dImsmeans)
ylabel('displacement')
title('Percentage of pixels going in the average direction compared to contractions')
[corr,pcorr]=corrcoef(mien,abs(dImsmeans)); % correlation between the % and the absolute value of the dotproduct
%% Subplots of each section
%{
woord='ABCDEFGHIJKL';
figure
title('Percentage going the "right" way on left axis compared to contractions over time')
for row = 1 : sectie
    subplot(vak, vak, row);
    % Do the plot.
    yyaxis left
    plot(t,percgoed(:,row))
    ylabel('%')
    yyaxis right
    plot(t,dImsec{row})
    ylabel('displacement')
    % Make it fancy.
```

```
    grid on;
    caption=sprintf('Section %d',row);
    title(caption, 'FontSize', 15);
end
%}
%% Cilinders
%{
teller0=1;
teller1=0;
teller2=0;
for i=1:vak
    for j=1:vak
        [X,Y,Z] = cylinder(percgoed(:,teller0)
    /100);
        surf(Z*119,X+teller1,Y+teller2)
        xlabel('time')
        ylabel('Percentage')
        zlabel('Percentage')
        %axis([0 120 -1 7 -1 7])
        teller1=teller1+3;
        hold on
        teller0=teller0+1;
        title('Percentage of correct angles for
    each section over time')
    end
    teller2=teller2+3;
    teller1=0;
end
%}
%% Quiver plot
%{
tic
[hoi1,hoi2] = meshgrid(1:vak,1:vak);
%plot(hoi1,hoi2,'.',X_sectie(:,:,1),Y_sectie
    (:,:,1),'-')
figure(2)
f(t_res+1) = struct('cdata',[],'colormap',[]);
f(1) = getframe(gcf);
for j = 1:t_res
    quiver(hoi1,hoi2,x_sectie(:,:,j),y_sectie(:,:,
    j),'r');
    axis([0 vak+1 0 vak+1])
    pbaspect([1 1 1])
    grid on
    drawnow
    f(j+1) = getframe(gcf);
end
str = sprintf('Filmpje_%1.0f.avi',G/1000);
v = VideoWriter(str);
open(v)
writeVideo(v,f)
close(v)
% movie2avi(F,'Filmpjie')
tee(8)=toc;
%}
```

```
function [ Re,Phie,dX ] = Tiff2mat(R_file,Phi_file
    ,x_res,y_res,t_res)
R=zeros(y_res,x_res,t_res); %initialize the
    flowvector radius array
Phi=zeros(y_res,x_res,t_res); %initialize the
    flowvector angle array
stop=size(R);
for i=1:stop(3) %Make x*y*t matrix for both
    flowvectors
    R(:,:,i)=imread(R_file,i); %Read the tiff file
     such that all frames get put into the matrix
    Phi(:,:,i)=imread(Phi_file,i);
end
Re=R;
Phie=Phi;
dX=nansum(nansum(R)); %Sum the displacement of all
     pixel per time frame,Assuming the PDMS gets
    stretched as far as the cells move
dX=dX(:); %change b from 1*1*#frames to #frames*1
end
```

```
function [ improduct, daim ] = improduct(X,Y,
    arb_vec,t_res,y_res,x_res)
improduct1=zeros(x_res,y_res,t_res);
for k=1:t_res
    for j=1:x_res
        for i=1:y_res
            improduct1(i,j,k)=X(i,j,k)*arb_vec(1)+
    Y(i,j,k)*arb_vec(2);
        end
    end
end
daim=nansum(nansum(improduct1));
daim=daim(:);
improduct=improduct1;
end
```

```
function [ Placeholder1 ] = sectionsum(matrix,
    secties,frames)
%UNTITLED Summary of this function goes here
%   Detailed explanation goes here
vak=sqrt(secties);
aantal=length(matrix);
b=aantal/vak;
Placeholder1=zeros(vak,vak,frames);
i3=0:(vak-1);
i2=1:vak;
% For loops delen de matrix op in # vakken
for i=1:vak
    for j=1:vak
        Placeholder1(i,j,:)=nansum(nansum(matrix((
    i3(i)*b+1):i2(i)*b,(i3(j)*b+1):i2(j)*b,:)));%
    end
end
end
```

```
function [ Placeholder2 ] = sectionmean(matrix,
    secties,frames)
vak=sqrt(secties);
aantal=length(matrix);
b=aantal/vak;
Placeholder2=zeros(vak,vak,frames);
cellsec=cell(16,1);
i3=0:(vak-1);
i2=1:vak;
% For loops delen de matrix op in # vakken
for i=1:vak
    for j=1:vak
        Placeholder2(i,j,:)=nansum(nansum(matrix((
    i3(i)*b+1):i2(i)*b,(i3(j)*b+1):i2(j)*b,:)));%
    end
end
Placeholder2=Placeholder2./(b^2);
end
```

```
%% Define some variables

close all; clearvars; pause on;
frames=120;
fram=frames-1;
```

```
fps=24;
t=1:fram;
tijd=t./24;
secties=16;
vak=sqrt(secties);
% arb_vec(1,:)=[0;1];
% arb_vec(2,:)=[1;0];
arb_vec(1,:)=[sqrt(2)/2;sqrt(2)/2];%arbitrair gekozen vector 45 graden 1 lang
% arb_vec(4,:)=[1/2;sqrt(3)/2];
% arb_vec(5,:)=[sqrt(3)/2;1/2];

%% Import data

[filename, foldername] = uigetfile({'*.*'}, 'Select File containing filtered tracks');
if filename~=0
    trackfile=fullfile(foldername, filename);
end
[filename2, foldername2] = uigetfile({'*.*'}, 'Select File containing track lengths');
if filename~=0
    lengthfile=fullfile(foldername2, filename2);
end
tracks=importdata(trackfile);
lengths=(importdata(lengthfile))';
if sum(lengths)~=length(tracks)
    [filename3, foldername3] = uigetfile({'*.*'}, 'Select File containing grouped detection');
    if filename~=0
        lengthfile2=fullfile(foldername3, filename3);
        lengthss=(importdata(lengthfile2))';
        if size(lengths)==size(lengthss)
            lengthss=lengthss;
        end
    end
end

%%

tracks=importdata('ParticleTrack15kPa\tracks.simple.filtered.txt');
lengths=importdata('ParticleTrack15kPa\results.track.length.txt');

%% Define some things

numtracks=length(lengths);
full_ind=(find((lengths==120))-1);%track identifier number of the tracks that span the whole width
numtracksall=length(full_ind); %number of tracks that span all frames
perc=sum(lengths==frames)/length(lengths)*100; %percentage of tracks that span the whole movie

%% Make cell with all tracks

tracksincells=mat2cell(tracks,lengths',8); %put all tracks in cells
tracksincells_og=tracksincells;
for i=1:numtracks %Make each cell the correct dimension
    nanan=nan(frames,8);
    a=tracksincells{i};
    start=a(1,1);
    nanan((start+1):(start+length(a)),1:8)=a;
    tracksincells{i}=nanan;
end

%% Make cell with only the tracks that span the full video

smallcells=cell(numtracksall,1);
teller=1;
for i=1:numtracks
    a=tracksincells_og{i};
    kak=length(a);
    if kak==frames
        smallcells{teller}=a;
        teller=teller+1;
    end
end

%% Make a new cell with each matrix only containing the X and the Y and then make them vectors

posincells = cellfun(@(tracksincells) tracksincells(:,2:3), tracksincells, 'UniformOutput', false);
shortposincells = cellfun(@(smallcells) smallcells(:,2:3), smallcells, 'UniformOutput', false);
vec_cell=cellfun(@diff,posincells,'UniformOutput', false); %get the vector between each frame
vec_cell_short=cellfun(@diff,shortposincells,'UniformOutput',false); %get the vector between each frame

%% Make cells with polar vectors, [theta, rho]

polar_cell=cell(numtracks,1);
polar_cell_short=cell(numtracksall,1);
rho=zeros(numtracks,fram);
x=zeros(numtracks,fram);
rho_short=zeros(numtracksall,fram);
theta=zeros(numtracks,fram);
y=zeros(numtracks,fram);

for j=1:numtracks
    [polar_cell{j}(:,1),polar_cell{j}(:,2)] = cart2pol(vec_cell{j}(:,1),vec_cell{j}(:,2));
    polar_cell{j}(:,3)=vec_cell{j}(:,3);
    a=(polar_cell{j}(:,2))';
    rho(j,:)=a;
    a=(polar_cell{j}(:,1))';
    theta(j,:)=a;
    a=vec_cell{j}(:,1);
    x(j,:)=a;
    a=vec_cell{j}(:,2);
    y(j,:)=a;
end

for j=1:numtracksall
    [polar_cell_short{j}(:,1),polar_cell_short{j}(:,2)]=cart2pol(vec_cell_short{j}(:,1),vec_cell_short{j}(:,2));
    a=(polar_cell_short{j}(:,2))';
    rho_short(j,:)=a;
end

dX_p=nansum(rho); %sum displacement
dX_p_short=nansum(rho_short);

%% Sectioning of the particletrack tracks only for all tracks

posi=cellfun(@nanmean ,posincells, 'UniformOutput', false);
```

```
posi=cell2mat(posi);
posi=[posi,zeros(numtracks,1)];
scatter(posi(:,1),posi(:,2))
title('Spread of tracked particles 15 kPa')
xrange=[min(posi(:,1));2048];
yrange=[min(posi(:,2));2048];
axis([0 2048 0 2048],'square')
[~,xbins] = histcounts(posi(:,1),vak);
[~,ybins] = histcounts(posi(:,2),vak);
LUT=flipud([7;49;343;2401].*ones(4,4)).*([1 2 3 4].*ones(4,4)); %translation table for the section number
for a=1:numtracks
    for i=1:vak
        for j=1:vak
            if posi(a,1)>=xbins(i)&&posi(a,1)<xbins(i+1)&&posi(a,2)>=ybins(j)&&posi(a,2)<ybins(j+1)
                posi(a,3)=i*7^j;
            end
        end
    end
end
sectienr=posi(:,3);
for i=1:numel(LUT)
    aiiiii=find(sectienr==LUT(i));
    sectienr(aiiiii)=i;
end
posi(:,3)=sectienr;
for i=1:numtracks
    vec_cell{i}(:,3)=sectienr(i)*ones(fram,1);
end
%% Cell to 3D array and cell containing the theta vectors for each section

thetatwee=cell(secties,1);
heey=cell2mat(polar_cell);
[r,c] = size(heey);
nlay  = length(heey)/fram;
out   = permute(reshape(heey',[c,r/nlay,nlay]),[2,1,3]);
drievecs= permute(out,[3 2 1]);
for k=1:secties
    b=drievecs(drievecs(:,3,1)==k,1,:);
    if isempty(b)==1
        thetatwee{k}=NaN;
    elseif isempty(b)==0
        thetatwee{k}=reshape(b,[numel(b)/fram,fram]);
    end
end
%% Take the improduct

i=1;
%for i=1:length(arb_vec)
[~,Im(i,:)]=improduct_part(vec_cell,numtracks,arb_vec(i,:),fram);
[~,Im_short(i,:)]=improduct_part(vec_cell_short,numtracksall,arb_vec(i,:),fram);
%end

%% Plot the improducts

%axis([0 frames/fps -1.1*min(dIm) 1.1*max(dIm)])
subplot(2,1,2)
plot(tijd,Im)
xlabel('Time(s)')
ylabel('Displacement')
title('Improducts summed')
subplot(2,1,1)
plot(tijd,dX_p)
xlabel('Time(s)')
ylabel('Displacement')
title('Absolute displacement summed')

%% Circular mean (unweighed average angle) & number of angles in the right direction

av_ang=zeros(fram,1);
bins=4;
for i=1:fram
    ph=polarhistogram(theta(:,i),bins);
    edges=ph.BinEdges;
    count=ph.BinCounts;
    av_ang(i)=atan2(nansum(sin(theta(:,i))),nansum(cos(theta(:,i))));
    ph2=polarhistogram(av_ang(i),edges);
    count2=ph2.BinCounts;
    ind=find(count2~=0);
    totaal=sum(count);
    goed=count(ind);
    percgoedal(i)=(goed./totaal).*100;
end

%% Circular StDev only applied to unweighed angles

n=length(theta);
R=sqrt((nansum(cos(theta))).^2+(nansum(sin(theta))).^2);
R_av=R/n;
c_std=sqrt(-2*log(R_av));
c_disp=(1-R_av)./(2*R_av);
%% Resultant vector

res_x=nansum(x);
res_y=nansum(y);
[res_theta,res_rho]=cart2pol(res_x,res_y);

%% Correlation between percgoed en improduct check normality
%{
%are they normally distributed?
pg=percgoed;
test_dist_pg=makedist('Normal','mu',mean(pg),'sigma',std(pg));
test_dist_im=makedist('Normal','mu',mean(Im),'sigma',std(Im));
thr=kstest(Im,'CDF',test_dist_im);
thre=kstest(pg,'CDF',test_dist_pg);
if thr==0 && thre==0
    %plot the cdf vs normal cdf
    [f,fx] = ecdf(pg);
    %[fa,fax] = ecdf(Im);
    figure(1)
    F = plot(fx,f);
    set(F,'LineWidth',2);
    hold on;
    G = plot(fx,normcdf(fx,mean(pg),std(pg)));
    set(G,'LineWidth',2);
    legend([F G],...
        'Empirical CDF','Standard Normal CDF',...
        'Location','SE');
    title('Improduct CDF vs normal CDF')
    figure(2)
    [fa,fax] = ecdf(Im);
    F = plot(fax,fa);
    set(F,'LineWidth',2);
    hold on;
    G = plot(fax,normcdf(fax,mean(Im),std(Im)));
    set(G,'LineWidth',2);
```

```
    legend([F G],'Empirical CDF','Standard Normal CDF','Location','SE');
    title('Improduct CDF vs normal CDF')
end
%}
%% Correlation between the improduct and the percentage of "correct" angles
%{
yyaxis left
plot(t,abs(Im));
yyaxis right
if thre==0
    plot(t,percgoed);
    title('|Improduct| in blue and percentage of vectors going the "right" direction in red')
    if kstest(Im,'CDF',test_dist_im)==0 && kstest(pg,'CDF',test_dist_pg)==0
        [coef,pval]=corrcoef(percgoed,abs(Im));
        if pval(1,2)<0.05
            fprintf('The correlation is %3.2f and significant',coef(1,2))
        end
    end
elseif kstest(pg,'CDF',test_dist_pg)==1
    plot(t,c_std);
    title('|Improduct| in blue and std of the vectors in red')
    if kstest(Im,'CDF',test_dist_im)==0
        [coef,pval]=corrcoef(c_std,abs(Im));
        if pval(1,2)<0.05
            fprintf('The correlation is %3.2f and significant',coef(1,2))
        end
    end
end
%}
%% Period and frequency of the contractions

[ac,lags]=xcorr(Im); %crosscorrelate with itself
[peaks,locs,w]=findpeaks(ac,fps,'MinPeakHeight',0.1*max(ac),'MinPeakProminence',0.1*max(ac)); %find the heights,times,widths and  of maxima of correlation
place1=[peaks,locs,w]; %place the findpeaks values into 1 matrix
place3=diff(locs); %finFor d the difference between each 2 neighbours
Period=[nanmean(place3),nanstd(place3)]; %take the mean of the differences, and multiply by the step size
Frequency=1./Period(1);
%% Histograms per section

clearvars cellplaats av_ang percgoed tid ph edges count ph2 count2 ind count2 ind totaal goed
cellplaats=cell(16,1);
av_ang=zeros(fram,16);
percgoed=zeros(fram,16);
bins=4;
for j=1:secties
    for i=1:fram
        tid=thetatwee{j};
        ph=polarhistogram(tid(:,i),4);
        count=ph.BinCounts;
        edges=ph.BinEdges;
        av_ang(i,j)=atan2(nansum(sin(tid(:,i))),nansum(cos(tid(:,i))));
        if av_ang(i,j)>=edges(1)&&av_ang(i,j)<=edges(5)
            edges=edges;
        else
            ph3=polarhistogram(tid(:),4);
            edges=ph3.BinEdges;
        end
        ph2=polarhistogram(av_ang(i,j),edges);
        count2=ph2.BinCounts;
        ind=find(count2~=0);
        totaal=sum(count);
        goed=count(ind);
        percgoed(i,j)=(goed./totaal).*100;
        if isnan(tid)==1
            break
        end
    end
    cellplaats{j}=percgoed;
end
%% Number of element per section and weighed percentage
sizes_sec=cellfun(@size,thetatwee,'UniformOutput',false);
elements_sec=cellfun(@(zzz) zzz(1),sizes_sec);
perc_weighed=(percgoed*elements_sec)/sum(elements_sec);
yyaxis left
plot(tijd,perc_weighed)
ylabel('%')
yyaxis right
plot(tijd,abs(Im))
ylabel('displacement')
title('Percentage of pixels going in the average direction vs abs(improduct)')
[corr,pcorr]=corrcoef(perc_weighed,abs(Im));
%% 3D plot the percentage of correct angles over time for each section
%{
plot3(repmat(t',1,secties),repmat(1:secties,numel(t'),1),percgoed)
title('Percentage of correct angles for each section over time')
%}
%% Plot cylinders for percentage for each section
%{
teller0=1;
teller1=0;
teller2=0;
for i=1:vak
    for j=1:vak
        [X,Y,Z] = cylinder(percgoed(:,teller0)/100);
        surf(Z*119,X+teller1,Y+teller2)
        xlabel('time')
        ylabel('Percentage')
        zlabel('Percentage')
        %axis([0 120 -1 7 -1 7])
        teller1=teller1+3;
        hold on
        teller0=teller0+1;
        title('Percentage of correct angles for each section over time')
    end
    teller2=teller2+3;
    teller1=0;
end
%}
%% test if the contractions from optic & parttrack come from the same dist
%h = kstest2(x1,x2)
```

```
function [ improduct2, dIm2 ] = improduct_part(
    vec_cell,Numtracks,arb_vec,fram)
improduct2=cell(Numtracks,1);
for k=1:Numtracks
    for i=1:fram
        improduct2{k}(i)=vec_cell{k}(i,1)*arb_vec
    (1)+vec_cell{k}(i,2)*arb_vec(2);
    end
end
improduct2=cell2mat(improduct2);
dIm2=nansum(improduct2);
end
```

```
function [ improduct, daim ] = improductcell(X,Y)
arb_vec=[sqrt(2)/2;sqrt(2)/2];
t_res=119;
y_res=292;
x_res=292;
for k=1:t_res
    for j=1:x_res
        for i=1:y_res
            improduct1(i,j,k)=X(i,j,k)*arb_vec(1)+
    Y(i,j,k)*arb_vec(2);
        end
    end
end
daim=nansum(nansum(improduct1));
daim=daim(:);
improduct=improduct1;
end
```

```
function [Frequency,Period,place3,place2,place1] =
     Periodcalc( dX, fps )
ac=xcorr(dX); %crosscorrelate with itself
[peaks,locs,w]=findpeaks(ac,fps); %find the
    heights,times,widths and  of maxima of
    correlation
place1=[peaks,locs,w]; %place the findpeaks values
     into 1 matrix
gem=mean(place1(:,3));%take the mean of the widths
for i=1:length(peaks) %if the peak is wider than
    the average width, keep the values, else
    replace all by inf(arbitrarily chosen to be
    able to remove)
    if place1(i,3)>gem
        place1(i,3)=place1(i,3);
    else
        place1(i,:)=inf;
    end
end
place2=setdiff(place1(:,2), inf); %remove the inf
    values, move them down, replace by nan
place3=diff(place2); %find the difference between
    each 2 neighbours
Period=[mean(place3),median(place3),std(place3)];
    %take the mean and std of the differences, and
     multiply by the step size
Frequency=1/Period;
end
```

```
clearvars; close all;
cd('C:\BEP\MATLAB');
[filename, foldername] = uigetfile({'*.*'}, '
    Select File R');
if filename~=0
    r_file=fullfile(foldername, filename);
else
    quit
end
[filename2, foldername2] = uigetfile({'*.*'}, '
    Select File Phi');
if filename~=0
    phi_file=fullfile(foldername2, filename2);
end
prompt = {'X resolution','Y resolution','Number of
     frames','FPS'};
dlg_title = 'Input';
num_lines = 1;
defaultans = {'2048','2048','200','20'};
answer1 = inputdlg(prompt,dlg_title,num_lines,
    defaultans);
answer=str2double(answer1);
%% Read the tiff files and sum the displacement
x_res=answer(1);
y_res=answer(2);
t_res=answer(3);
[r,phi,dX] = Tiff2mat(r_file,phi_file,x_res,y_res,
    t_res); %dX is in pixels
%% turn the polar matrices into cartesian
tic
[x,y]=pol2cart(phi,r);
tee(2)=toc;
%% Plot force/displacement
t=1:t_res;
plot(t,movmean(dX,5))
axis([0 t_res 0.8333*min(dX) 1.2*dX(end)])
title('Contraction of a single VSMC due to KCl
    addition')
xlabel('Time')
ylabel('Displacement')
```

```
periods = [1.55 1.646;1.306 2];
stds = [0.0349 0.024; 0.0776 4.4E-16];
h = bar(periods);
set(h,'BarWidth',1);    % The bars will now touch
    each other
set(gca,'YGrid','on')
set(gca,'GridLineStyle','-')
set(gca,'XTicklabel',{'15 kPa','100 kPa'})
set(get(gca,'YLabel'),'String','Period observed (s
    )')
lh = legend('Optic flow','Particle tracking');
set(lh,'Location','BestOutside','Orientation','
    horizontal')
hold on;
numgroups = size(periods, 1);
numbars = size(periods, 2);
groupwidth = min(0.8, numbars/(numbars+1.5));
for i = 1:numbars
      x = (1:numgroups) - groupwidth/2 + (2*i-1) *
     groupwidth / (2*numbars);  % Aligning error
    bar with individual bar
      errorbar(x, periods(:,i), stds(:,i), 'k', '
    linestyle', 'none');
end
```